Neurobiology of Disease

Altered Response Dynamics and Increased Population Correlation to Tonal Stimuli Embedded in Noise in Aging Auditory Cortex

Kelson Shilling-Scrivo,[1]* Jonah Mittelstadt,[2]* and Patrick O. Kanold[2,3,4]

[1]Department of Anatomy and Neurobiology, University of Maryland School of Medicine, Baltimore, Maryland 21230, [2]Department of Biology, University of Maryland, College Park, Maryland 20742, [3]Department of Biomedical Engineering, Johns Hopkins University, Baltimore, Maryland 20215, and [4]Kavli Neuroscience Discovery Institute, Johns Hopkins University, Baltimore, MD 21205

Age-related hearing loss (presbycusis) is a chronic health condition that affects one-third of the world population. One hallmark of presbycusis is a difficulty hearing in noisy environments. Presbycusis can be separated into two components: alterations of peripheral mechanotransduction of sound in the cochlea and central alterations of auditory processing areas of the brain. Although the effects of the aging cochlea in hearing loss have been well studied, the role of the aging brain in hearing loss is less well understood. Therefore, to examine how age-related central processing changes affect hearing in noisy environments, we used a mouse model (Thy1-GCaMP6s X CBA) that has excellent peripheral hearing in old age. We used *in vivo* two-photon Ca^{2+} imaging to measure the responses of neuronal populations in auditory cortex (ACtx) of adult (2–6 months, nine male, six female, 4180 neurons) and aging mice (15–17 months, six male, three female, 1055 neurons) while listening to tones in noisy backgrounds. We found that ACtx neurons in aging mice showed larger responses to tones and have less suppressed responses consistent with reduced inhibition. Aging neurons also showed less sensitivity to temporal changes. Population analysis showed that neurons in aging mice showed higher pairwise activity correlations and showed a reduced diversity in responses to sound stimuli. Using neural decoding techniques, we show a loss of information in neuronal populations in the aging brain. Thus, aging not only affects the responses of single neurons but also affects how these neurons jointly represent stimuli.

Key words: **aging; auditory cortex; correlation; noise; offset; population**

Significance Statement

Aging results in hearing deficits particularly under challenging listening conditions. We show that auditory cortex contains distinct subpopulations of excitatory neurons that preferentially encode different stimulus features and that aging selectively reduces certain subpopulations. We also show that aging increases correlated activity between neurons and thereby reduces the response diversity in auditory cortex. The loss of population response diversity leads to a decrease of stimulus information and deficits in sound encoding, especially in noisy backgrounds. Future work determining the identities of circuits affected by aging could provide new targets for therapeutic strategies.

Introduction

The inability to hear speech in complex auditory environments is a defining feature of age-related hearing loss. Human studies have shown that aging subjects with intact peripheral auditory systems perform worse on gap detection, sound source localization, and temporal perception, indicating a deficiency of central processing (Fitzgibbons and Gordon-Salant, 1998; Gordon-Salant and Fitzgibbons, 1999; Lister et al., 2002; Wambacq et al., 2009). Factors that contribute to hearing difficulty in healthy aging can broadly be grouped into two main categories, peripheral degeneration of the auditory transduction mechanisms in the ear (Gopinath et al., 2009; Lin et al., 2011) and changes in the central auditory processing areas that decode those peripheral signals (Caspary et al., 2008; Cisneros-Franco et al., 2018).

One complicating factor in understanding the central effects of aging is separating them from peripheral effects. Animal studies have shown that age-related high-frequency hearing loss can lead to remapping of central auditory brain regions such as the inferior colliculus and auditory cortex (ACtx; Reale et al., 1987;

Received Apr. 18, 2021; revised Sep. 25, 2021; accepted Sep. 29, 2021.

Author contributions: P.O.K. and K.S.-S. designed research; K.S.-S. and J.M. performed research; K.S.-S. and J.M. analyzed data; P.O.K. and K.S.-S. wrote the paper.

This work was supported by the National Institute on Aging Grant P01 AG055365 (P.O.K.), the National Institutes of Health Grant RO1DC009607 (P.O.K.) and National Institutes of Health Grant T32DC000046 (K.S.-S.). We thank Nik Francis, Zac Bowen, Travis Babola, and Ji Liu for technical help.

*K.S.-S. and J.M. contributed equally to this work.

The authors declare no competing financial interests.

Correspondence should be addressed to Patrick O. Kanold at pkanold@jhu.edu.

https://doi.org/10.1523/JNEUROSCI.0839-21.2021

Robertson and Irvine, 1989; Schuknecht and Gacek, 1993; Pasic et al., 1994; Harrison et al., 1998; Mendelson and Ricketts, 2001; Mendelson and Lui, 2004; Gourévitch and Edeline, 2011; Dubno et al., 2013; Engle et al., 2013; Trujillo and Razak, 2013; Recanzone, 2018; Park et al., 2019). In particular, mice of the C57BL/6 strain show peripheral hearing loss in young adulthood, with hearing impairment becoming evident during 8–12 months of age (Henry and Chole, 1980). C57BL/6 mice show a remapping of ACtx in response to peripheral hearing loss (Willott et al., 1993). Thus, to identify the central effects of aging, it is critical to use a model that has an intact peripheral auditory system. One such model are CBA mice, which have good peripheral hearing into old age (Willott et al., 1988, 1991; Bowen et al., 2020) and thus allow distinguishing remapping effects from other consequences of aging on central auditory neurons.

In healthy animals, central auditory areas, such as ACtx, robustly encode target sounds in a noisy background (Ulanovsky et al., 2004; Rabinowitz et al., 2013; Natan et al., 2015), and it is thought that ACtx is critical for detecting natural and complex stimuli in noise (Rabinowitz et al., 2013; Teschner et al., 2016; Downer et al., 2017; Malone et al., 2017). Indeed, decreasing signal-to-noise ratio (SNR) decreases neural responses to tones in single neurons in thalamorecipient layers (layer four or L4) of primary ACtx (A1; Teschner et al., 2016). However, the age-related changes that occur in tone-in-noise processing in ACtx are unknown.

To understand how A1 processes tones in noise and how this processing changes with age, we imaged ~5000 neurons from Thy1-GCaMP6s X CBA mice (young, 2–6 months old; aged 15–17 months old) using *in vivo* two-photon (2P) Ca^{2+} imaging while presenting tones (4–32 kHz, 50–70 dB SPL) embedded in broadband noise (50 dB SPL). We found that neurons in aging animals have increased responsiveness to sound and fewer suppressed responses than neurons in young animals. We also found that neurons in aging animals have fewer responses to sound offset and fewer neurons responsive to tone onset in noise. Using population measures, we found that aging mice showed a reduced diversity of neuronal functional responses and that neurons had higher activity correlations. Finally, using a Bayesian decoder, we found that these changes in population activity led to a loss of tone information.

Materials and Methods

Animals. All procedures were approved by the University of Maryland Institutional Animal Care and Use Committee. We used 24 mice total with a cohort of 15 young animals (nine male, six virgin female, 3–6 months) and a cohort of 9 aging animals (six male, three virgin female, 15–17 months). Thy1-GCaMP6s (stock #024275, The Jackson Laboratory) were used for 2P calcium imaging of cortical neurons. We crossed these mice with CBA/CaJ mice (stock #000654, The Jackson Laboratory), which are known for exceptional hearing in these mice (Parham and Willott, 1988), to create Thy1-GCaMP6s X CBA mice. We tested all mice for the early hearing loss mutation *Cdh23*^{Ahl,} a recessive allele that causes early onset hearing loss in mice. All mice used in the study had at least one copy of WT allele, ensuring normal hearing. Mice were housed in a 12 h light/dark cycle room.

Surgery. Mice were prophylactically injected with dexamethasone (5 mg/kg) 2 h before surgery to prevent infection and cortical edema. Mice were anesthetized with isoflurane (3–4% for induction, 1.5–2% for maintenance). Internal body temperature was maintained at 38°C using a heating pad with a closed loop homeothermic monitoring system. At the time of surgery, mice were injected again with dexamethasone and atropine (0.1 mg/kg). Hair was removed via plucking and hair removal agent (Nair). The scalp was then disinfected with three alternating swabs of betadine and 70% ethanol. The skin above the skull and temporal muscle was then removed, and the temporal muscle was resected to expose the temporal bone. The head post was then attached to the skull with a combination of cyanoacrylate (Vetbond) and dental acrylic (C&B Metabond). A 3 mm circular section of bone above A1 was then removed and the cranial window was implanted. The cranial window consisted of two 3 mm circular glass coverslips affixed to one 5 mm circular coverslip, the edges of which were filled with a clear silicone elastomer (Kwik-Sil). The window was then affixed in place with the same dental acrylic. The dental acrylic and head post were then coated in iron oxide to prevent optical reflections. Mice were postoperatively given injections of meloxicam (0.5 mg/kg) and were allowed to recover for at least a week before experiments.

In vivo *two-photon imaging.* Imaging was performed in animals as described previously (Liu et al., 2019). After recovery and acclimatization to the microscope, AC location was functionally determined by its characteristic rostrocaudal tonotopic axis using widefield imaging (Liu et al., 2019). All experiments were performed on a rotatable microscope (Bergamo II series B248, Thorlabs) using a pulsed femtosecond Ti:Sapphire 2P laser (Vision S, Coherent) and ThorImage and ThorSync software. Imaging was performed at 940 nm excitation wavelength. The imaging field size was ~370 μm × 370 μm and was imaged at 30 frames per second.

Sound stimuli. All sound stimuli were presented with a free-field electrostatic speaker 10 cm away from the right ear of the mouse (ES1 speaker with ED1 speaker driver, TDT) The speaker was calibrated by first recording a 70 dB SPL, 4–64 kHz white noise with a calibrated microphone to find the natural transfer function of the speaker. We then calculated the inverse of the function, which when added to the natural transfer function of the speaker, will equalize the output of the speaker, giving a flat frequency/dB curve. We then tested this calibration by recording pure tones at 70 dB SPL and ensured that the recorded sound level was <5 dB from the target for all tones played. During 2P imaging, 1 s sinusoidally amplitude-modulated tones (4–32 kHz, one-half-octave spacing, 5 Hz full-depth modulation) at 70, 60, and 50 dB SPL were presented together with a constant (4–48 kHz 50 dB SPL) broadband white noise to obtain SNRs of +20, +10, and 0 dB, respectively. Each trial consisted of a 1 s prestimulus silence, followed by 1 s of white noise, 1 s of tone presented in white noise, and then 1 s of white noise alone, and a 1 s poststimulus silence (Fig. 1*A*, inset). To compare these tone-in-noise responses to traditional measures, we also played the 70 dB tone in quiet as the infinite SNR condition. These stimuli were randomly interleaved with a variable 6–10 s intertrial interval between stimuli. Each unique frequency/SNR combination was presented for 10 repeats to increase statistical confidence for a total of 320 trials.

Imaging data analysis. Neuron fluorescence traces were extracted using custom MATLAB code (MathWorks version 2016B; Francis et al., 2018). Images were motion corrected to subpixel precision using discrete time Fourier transforms (Guizar-Sicairos et al., 2008). Cell bodies were then manually selected with cell bodies and neuropil divisions created automatically (Chen et al., 2013). Any pixels that overlapped multiple cells were excluded from analysis. For each neuron, all pixels within the cell body were averaged to create the baseline fluorescence (F) value. To calculate the neuropil fluorescence, all pixels in a ring surrounding the labeled neuron were averaged, excluding pixels that corresponded to other neurons. The corrected neuropil fluorescence was calculated as follows: $F_{Cell\_Corrected} = F_{Cell} - 0.7 * F_{Neuropil}$. We calculate df/F by dividing fluorescence from each trial by the average F of the preceding silent baseline frames. To test whether neurons were responsive to sound, we performed an ANOVA of sound frames before and after sound presentation. Neurons were considered sound responsive if the fluorescence of the neurons after sound presentation was statistically different from baseline fluorescence.

Statistics. All significance testing was performed using built-in MATLAB functions unless otherwise noted. All one-way ANOVAs were calculated using the anova1 function. Higher order ANOVAs (indicated by VARIABLE_1 X VARIABLE_2 notation in text) were calculated using the anovan function. Multiple comparisons were corrected for using the multcompare function on the results of the ANOVA. Multiple comparisons were performed using Tukey's honest significant difference

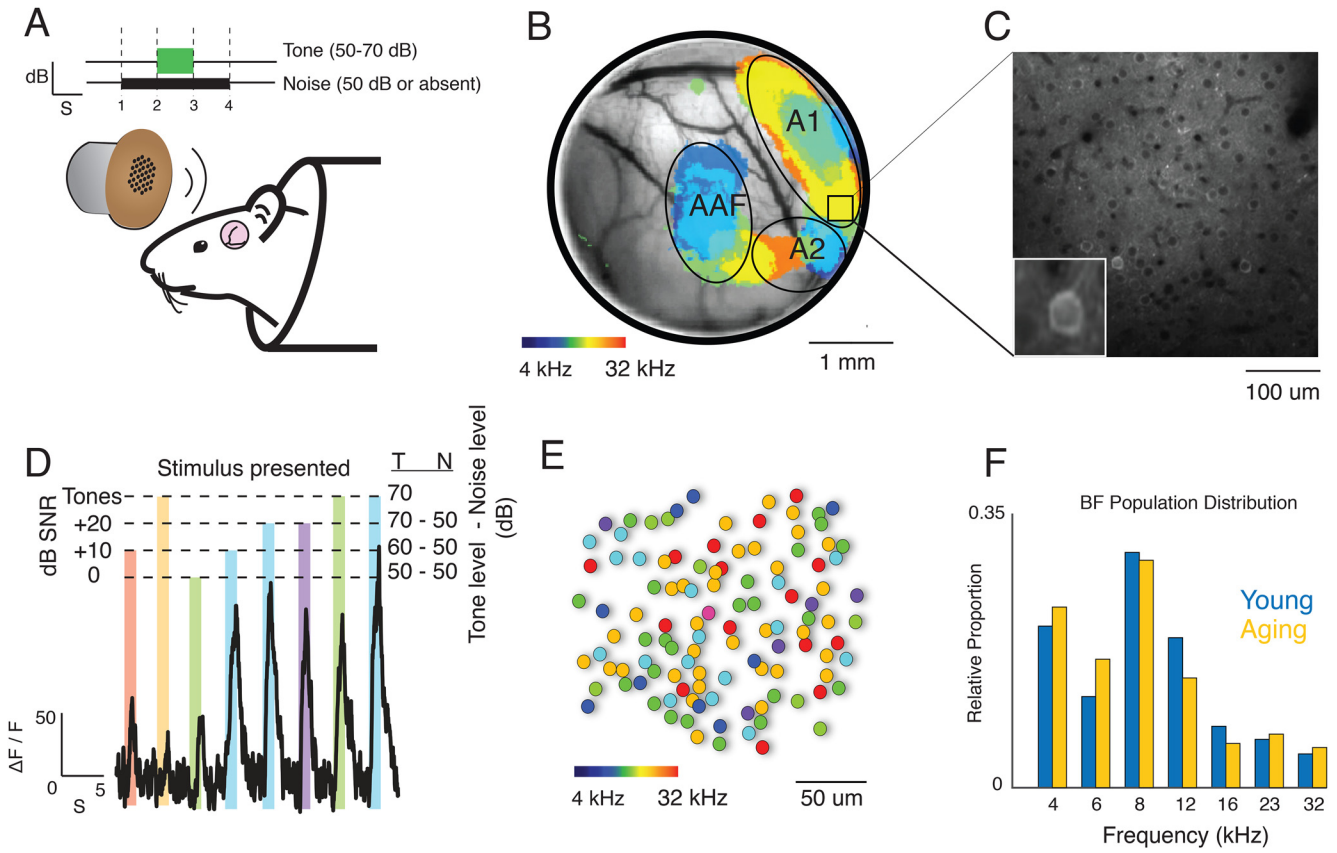

Figure 1. *In vivo* imaging of A1 in young adult and aging mice. ***A***, Mouse A1 was imaged using 2P microscopy while passively listening to tones in noise from a single speaker positioned 10 cm from the contralateral ear. ***B***, Example cranial window. Colors indicate the best frequency of that region. A1 is then identified and subdivided based on its stereotypical patterns of activity. ***C***, Typical 2P imaging field of view. Inset, Magnification of a single neuron. ***D***, Example trace from a neuron while presenting tones (4–32 kHz, one-half octave spacing) at one of four different SNRs. Bar color indicates frequency of tone played, bar height indicates the SNR of the trial, and bar width indicates stimulus duration. Tone and noise levels are given on the right. The SNR indicated as Tones is the reference Infinite SNR condition in which no noise is played. ***E***, Extracted neurons from a field of view. Color indicates BF of the neuron. ***F***, BF distributions of young and old neurons across all animals were similar.

unless otherwise noted. Student's *t* tests between group means were performed using the ttest2 function.

Intensity analysis. All measures of fluorescence intensity were performed during the tone presentation period. For each cell, we found the maximum response to tones and the average response to tones (labeled maximum and mean response, respectively).

Bandwidth analysis. To obtain bandwidth measures for each cell, the average response to each tone/sound level combination was calculated and normalized to the largest response. Responses were then interpolated at 0.1 octave spacing for smoothing. To find the bandwidth for a given level, we found the distance in octaves between the two frequencies at 50% of the maximum response. For multipeaked neurons, only the bandwidth of the largest peak was calculated. This was repeated to find the bandwidth for each neuron at each sound level.

Signal/noise correlations. Signal/noise correlations were calculated as in Winkowski and Kanold (2013). The signal correlation is defined as how similar (and thus correlated) the tuning curves are for two neurons. We obtain the tuning curve for a single neuron by calculating the average response to each tone/level combination across trials. Tuning curves were calculated for each neuron to create a N × M matrix where N corresponds to the number of neurons, and M is the unique combination of tone/level combinations. To obtain the correlations between two neurons (i and j), we obtained the correlation between the tuning curves we used the Pearson correlation equation as follows:

$$Corr_{ij} = \frac{Cov_{ij}}{\sqrt{Var_{ii} * Var_{jj}}}.$$

Neurons with direct connections to each other or that share common inputs will show correlated trial-to-trial activity. Noise correlations are defined as any trial-to-trial correlated activity that is not explained by signal correlations. To obtain noise correlations, we first found the average fluorescence response during each trial. To remove the effect of signal correlations, we subtracted the average response of the cell to that stimulus, leaving only the trial-to-trial variance. Calculating this for each neuron we created an N × M matrix, where N is the number of neurons and M is the deviation from the average response of the neuron on each trial. From this noise matrix, we calculated the trial-to-trial correlation between each pair of neurons with the same Pearson correlation equation above. We analyzed significance by creating a two-way Age × SNR ANOVA with corrections for multiple comparisons.

Naive Bayes modeling. The naive Bayes decoder uses Bayes's rule to determine which tone was played given the neural activity of a subset of neurons. Data were in the form of a time × trial × neuron matrix. For each time point, a random subset of neurons was selected for the model and used to create a naive Bayes model using the MATLAB function fitcnb. Confidence intervals were determined by running 10 such models and plotting the mean and 95% confidence intervals. See the following for a detailed description of the mathematics behind naive Bayes.

The probability that a tone was played given a certain neural population activity can be written as follows:

$$P(Tone|Neural\,Activity) = \frac{P(Neural\,Activity|Tone)P(Tone)}{P(Neural\,Activity)},$$

where P (Neural Activity|Tone) is modeled as random draws from a Gaussian distribution as follows:

$$P(Neural\ Activtity|Tone) = \frac{1}{\sqrt{2\pi^2}} * exp(\frac{(X-\mu)^2}{-2\sigma^2}),$$

where μ and σ represent the mean and SD of the neural activity.

The model therefore takes the neural activity of each trial, calculates the probabilities that each of the tones generated that neural activity, and predicts the class with the largest associated probability as in the following:

$$Y = Argmax\begin{pmatrix} P(Tone_i|Neural\ Activity) \\ \vdots \\ P(Tone_n|Neural\ Activity) \end{pmatrix}.$$

To ensure the validity of the model, it is run with 10-fold cross validation. The model is rerun five times using different random subsets of training data to ensure accurate model performance.

Temporal analysis. We began with a time × trial × neuron matrix, where each index represents the calcium activity of a neuron on that time point and trial. We first obtained the average response for each neuron by averaging each neuron response across trials to create a time × neuron matrix. To show how the response of the neuron changed over time, we then took the approximate derivative of the response of each neuron with the MATLAB diff function. Then, for each neuron we found the time point for when the maximum change in response occurred. We binned these response times for greater statistical power and used a one-way ANOVA with multiple comparisons to determine time points that had a significant number of cells compared with silence (the first two time bins).

Clustering. We performed K-means clustering by using the k-means_opt function in MATLAB File Exchange (Sebastien De Landtsheer, 2021). To create the clusters, we used the average response of each neuron across trials in a time × neuron matrix. K-means clustering is an iterative algorithm cluster based on the Euclidean distance to the cluster center in high-dimensional space. To ensure stability, this process is then repeated twice more, with the best results taken as the cluster outputs. To determine the optimal number of clusters to use, we run the algorithm with an increasing number of clusters until the current clustering can explain 95% of the variance. For each animal, cluster diversity was calculated as the number of clusters with at least 5% of representation in the field of view.

Results

To investigate how age affects processing of tones in noisy backgrounds, we performed two-photon imaging of young adult mice (2–6 months, $N = 15$, 9 male, 6 female, 4180 neurons) and aging mice (15–17 months, $N = 9$, 6 male, three female, 1055 neurons) while presenting tones (4–32 kHz, 50–70 dB SPL) embedded in broadband noise (50 dB SPL; Fig. 1*A*). We used F1 offspring of Thy1-GCaMP6s mice (stock #024276, The Jackson Laboratory) crossed with CBA/CaJ mice (stock #000654, The Jackson Laboratory), which retain normal hearing thresholds into adulthood (Spongr et al., 1997; Frisina et al., 2011; Francis et al., 2018). We imaged each animal in L2/3 (depth, 150–300 μm) covering the low-to-mid frequency region of A1 (Fig. 1*B*,*C*).

Aging mice do not show reduction in auditory cortex cells responsive to high frequencies

As we aimed to identify central changes not because of peripheral hearing loss, we first confirmed that the aging mice used in this experiment showed similar neuronal distribution of frequency selectivity as young mice. If aging F1 mice did have a reduced hearing range because of peripheral neural degeneration, we would predict a shift in best frequency (BF) distribution toward the lower frequency neurons in A1, as is the case with C57/BL6 animals (Willott et al., 1993). We presented tones (4–32 kHz, 50–70 dB SPL) and obtained fluorescence traces for each imaged neuron (Fig. 1*D*). To obtain neuronal BFs, we calculated the average response to each tone across all SNR levels (Fig. 1*D*). Neurons that had significant change ($\alpha = 0.01$) in fluorescence during stimulus frames as compared with baseline frames were classified as sound responsive. Consistent with prior results in L2/3, BFs had a salt-and-pepper distribution. (Bandyopadhyay et al., 2010; Rothschild et al., 2010; Winkowski and Kanold, 2013; Kanold et al., 2014; Bowen et al., 2020). When plotting the BFs of all neurons as a histogram, we found that the overall BF distributions were similar between young and aging animals, with <5% change between the two on average (Fig. 1*F*). Thus, the representations between young and aging mice were similar for the frequencies and mouse model used in this experiment.

Neurons in aging A1 have higher average fluorescence amplitudes in response to sounds

We first examined the basic response properties of neurons by comparing the strength of sound-evoked responses both with pure tones without background and with the same pure tones in broadband noise (+20 dB SNR). Although we found no difference in maximum fluorescence responses to tones in quiet at the cell or animal level (Fig. 2*A*), we found that aging neurons have larger mean responses to tones (Student's *t* tones, maximum cell: $t = -1.17$, $p = 0.24$; maximum animal: $t = -1.72$, $p = 0.09$; mean cell: $t = 5.4$, $p = 3.2e\text{-}8$; mean animal: $t = -2.58$, $p = 0.017$). This effect continues in tones in noise, as aging neurons are more responsive in the +20 dB SNR condition (Fig. 2*B*; Student's *t* maximum cell: $t = -1.17$, $p = 0.085$; maximum animal: $t = -1.72$, $p = 0.098$; mean cell: $t = -5.53$, $p = 3.35e\text{-}8$; mean animal: $t = -2.57$, $p = 0.017$). Thus, A1 neurons in aging mice are more responsive to sound, and increased responsiveness is amplified by background noise.

Separating the animals by sex revealed a differential effect of aging. In males, the aging cohort had larger responses across all conditions (Fig. 2*C*,*D*). The females, however, had much more similar responses between age groups. There was no difference between animals in quiet (Fig. 2*E*; maximum, $p = 0.08$; mean, $p = 0.72$). In noise, young female animals had larger responses to tones for both maximum and mean responses than aging females at the cell level (Fig. 2*F*; Student's *t* tones, maximum cell: $t = 1.71$, $p = 0.086$; maximum animal: $t = -0.08$, $p = 0.86$; mean cell: $t = -0.33$, $p = 0.72$; mean animal: $t = -0.44$, $p = 0.67$; +20 dB maximum cell: $t = 2.49$, $p = 0.010$; maximum animal: $t = 0.08$, $p = 0.93$; mean cell: $t = 2.13$, $p = 0.032$; mean animal: $t = -0.44$, $p = 0.67$). Therefore, A1 neurons in aging male mice are more responsive to sound and that increased responsiveness is amplified by background noise.

Neurons in aging A1 have altered excited and suppressed receptive fields and altered bandwidth

The precise balance of excitation and inhibition is critical for proper neurotransmission. Studies in aging animals have shown disruptions of excitatory and inhibitory neurons, including decreased density of inhibitory synapses, reduced GAD levels, hypofunction of NMDAR, and reduced dendritic spine density (De Luca et al., 1990; Willott et al., 1993; Chaudhry et al., 1998; Milbrandt et al., 2000; Shi et al., 2004; Stanley and Shetty, 2004; Ling et al., 2005; Peters et al., 2008; Burianova et al., 2009; Stanley et al., 2012; Gold and Bajo, 2014; Liguz-Lecznar et al., 2015; Liao et al., 2016; Kumar et al., 2019). However, in these prior studies it is unclear how much of these changes are because of peripheral effects of cochlear hair cell loss. We thus aimed to

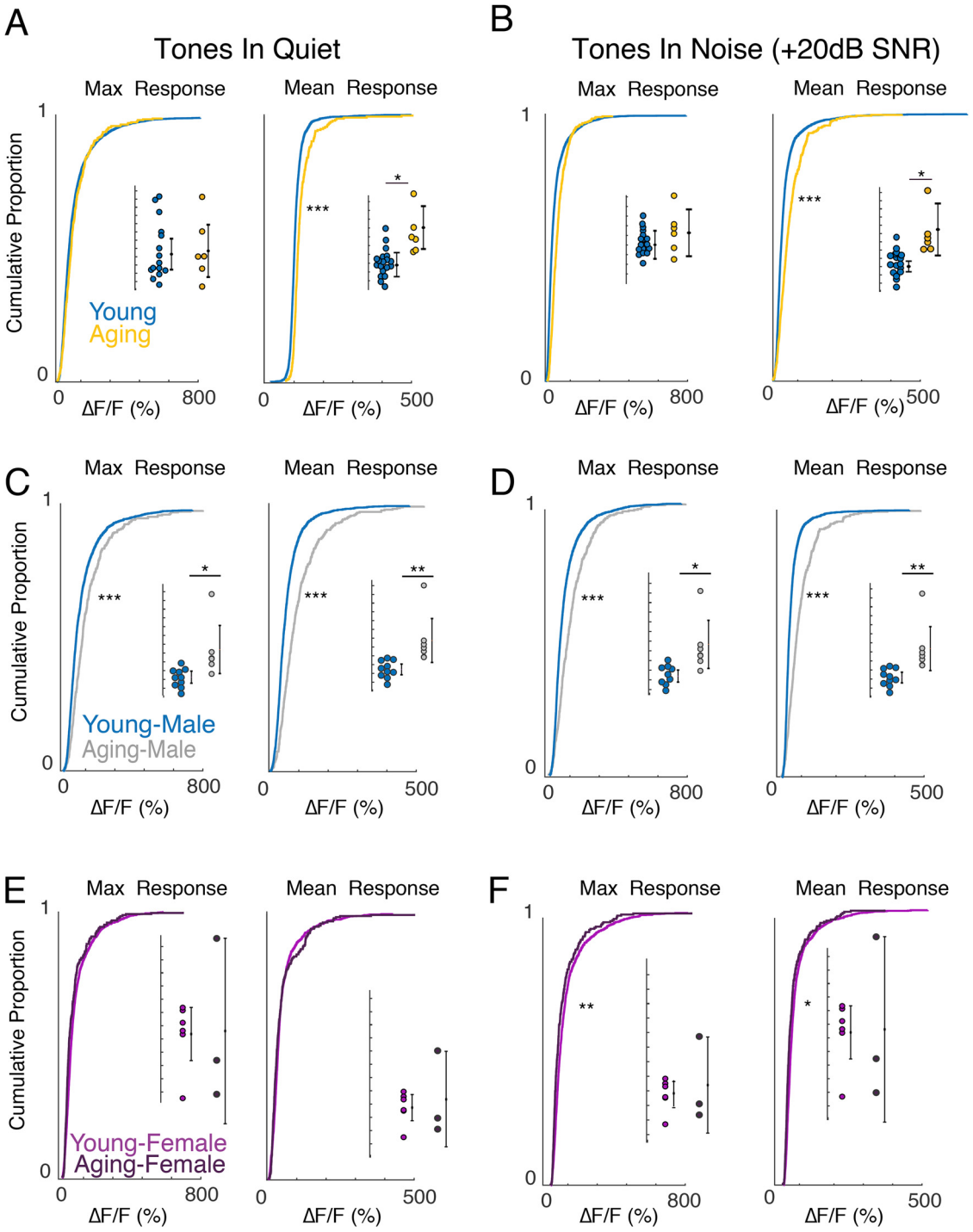

Figure 2. Aging neurons have larger responses to tones. ***A***, Cumulative distributions of the maximum (left) and mean (right) neuronal responses (ΔF/F) to tones in quiet. Insets, Average response by animal. Maximum response is defined as the maximum response evoked during tone presentation across trials. Mean response is defined as the average response to tones across trials. When tones were presented in quiet, aging animals have similar maximum responses (aging 115% ΔF/F, young 120% ΔF/F) and higher mean responses (aging 57.7% ΔF/F, young 47.7% ΔF/F) compared with younger animals at the cell and animal level (Student's *t* maximum cell, $t = -1.17$, $p = 0.24$; maximum animal, $t = -1.72$, $p = 0.09$; mean cell, $t = 5.4$, $p =$ 3.2e-8; mean animal, $t = -2.58$, $p = 0.017$). ***B***, Maximum (aging, 114% ΔF/F; young 123% ΔF/F) and mean (aging, 47.6% ΔF/F; young, 59.6% ΔF/F) neuronal responses (ΔF/F) to tones in 50 dB SPL white noise (maximum cell, $t = -1.17$, $p = 0.085$; maximum animal, $t = -1.72$, p = 0.098; mean cell, $t = -5.53$, $p =$ 3.35e-8; mean animal $t = -2.57$, $p = 0.017$). ***C–F***, Results separated by sex. ***C–D***, Aging males have significantly larger responses both in quiet (mean: aging 59.7% ΔF/F, young 41.5% ΔF/F; maximum: aging 135% ΔF/F, young 101% ΔF/F) and in noise (mean: aging 69.9% ΔF/F, young 42.3% ΔF/F; maximum: aging 123% ΔF/F, young 101% ΔF/F; tones: maximum cell, $t = -4.81$, $p =$ 7.72e-10; maximum animal, $t = -2.09$, $p = 0.05$; mean cell, $t = -10.6$, $p =$ 1.9e-33; mean animal, $t = -2.88$, $p =$0.012, +20 dB; maximum cell, $t = -6.67$, $p =$ 8.63e-15; maximum animal, $t = -2.09$, $p = 0.056$; mean cell, $t = -12$, $p =$ 1.37e-40). ***E–F***, Aging females have no significant change when tones are presented quiet and have smaller responses to tones in noise (mean: aging 45.1% ΔF/F, young 53.6% ΔF/F; maximum: aging 105% ΔF/F, young 128% ΔF/F) at the cell level (tones: maximum cell, $t = 1.71$, $p = 0.086$; maximum animal, $t = -0.08$, $p = 0.86$; mean cell, $t = -0.33$, $p = 0.72$; mean animal, $t = -0.44$ $p = 0.67$ + 20 dB; maximum cell, $t = 2.49$, $p = 0.010$; maximum animal, $t = 0.08$, $p = 0.93$; mean cell, $t = 2.13$, $p = 0.032$; mean animal, $t = -0.44$, $p = 0.67$).

identify how imaged neurons responded to changes in frequency and SNR. Given that we presented tones in the presence of background noise, we noted that some neurons had significant decreases in fluorescence in response to sound. Therefore, we further separated neurons by whether the average fluorescence of the neuron significantly increased or decreased during tone presentation and labeled them as excited and suppressed cells, respectively.

When comparing excited neuronal responses in young and aging animals, we find that neurons from young and aging animals had similar bandwidths in quiet and at the +20 dB SNR (Fig. 3*A*). However, as SNR is further decreased, neurons from aging animals had significantly smaller bandwidths (age × SNR ANOVA age * SNR interaction, $F_{(1,3)} = 9.05$, $p = 5.05e\text{-}6$; *post hoc* tests, tones: $p = 0.96$, +20: $p = 0.72$, +10: $p = 0.01$, 0: $p = 1.0e\text{-}4$). Comparing by sex, we find that male and females animals largely followed the same pattern with significant differences only occurring at lower SNRs (Fig. 3*B*; males, age × SNR ANOVA age * SNR interaction, $F_{(1,3)} = 8.12$, $p = 2.13e\text{-}5$; *post hoc* tests, tones: $p = 0.76$, +20: $p = 0.35$, +10: $p = 0.21$, 0: $p = 6.0e\text{-}4$; Fig. 3*C*; females, age × SNR ANOVA age * SNR interaction, $F_{(1,3)} = 4.03$, $p = 0.007$; *post hoc* tests, tones: $p = 0.99$, +20: $p = 0.44$, +10: $p = 0.03$, 0: $p = 0.24$). A1 receptive fields can be diverse with multiple peaks (Sutter and Schreiner, 1991; Liu and Kanold, 2021), and the bandwidth measure will only take into account the central region of the receptive field. To gain a more inclusive understanding of frequency integration, we thus also used an additional measure, the binary receptive field sum (BRFS; Bowen et al., 2020), which allows incorporation of frequency responses outside the central receptive field. At a single sound level, the BRFS is simply the sum of the frequency bins a neuron was responsive to (Fig. 3*C*). Plotting the BRFS for cells in young and aged animals shows similar results as the bandwidth measure (Fig. 3*J–L*) but also reveals differences. For example, aging males showed a smaller BRFS in quiet than young males. Because the bandwidth was similar, this suggests a decreased response to frequencies outside the central receptive field in aging mice.

We similarly compared suppressed responses in cells across all young and aging animals. Suppressed bandwidth was similar between groups (age * SNR interaction, $F_{(1,3)} = 1.60$, $p = 0.16$; *post hoc* tests, tones: $p = 0.92$, +20: $p = 0.68$, +10: $p = 0.99$, 0: $p = 0.96$; Fig. 4*A*). However, when we separate the animals by sex, we see significant effects. Cells from aging males (Fig. 4*B*) have a reduction in suppressed bandwidth in all noise conditions (age * SNR interaction, $F_{(1,3)} = 8.84$, $p = 7.73e\text{-}6$; *post hoc* tests, tones: $p = 0.98$, +20: $p = 1.0e\text{-}3$, +10: $p = 6.40e\text{-}8$, 0: $p = 6.20e\text{-}8$). Cells from aging females, (Fig. 4*C*) showed the opposite pattern, and have significantly larger suppressed bandwidths in noise ($F_{(1,3)} = 3.51$, $p = 0.01$, tones: $p = 0.58$, +20: $p = 0.011$, +10: $p = 5.99e\text{-}8$, 0: $p = 8.40e\text{-}3$). Investigating the effect of age on the animal level revealed that only females had a significant effect (Figure 4*D–F*; age × SNR ANOVA, effect of age, all: $F_{(1)} = 1.81$, $p = 0.179$; males: $F_{(1)} = 1.06$, $p = 0.30$; females: $F_{(1)} = 13.0$, $p = 1.2e\text{-}3$). Plotting the BRFS (Fig. 4,*G–I*) showed the similar pattern of decreased BRFS in noise for males and increased BRFS in noise for females. Together, these data show that suppressed sound responses are differentially altered with aging in aging males and females.

Increased activity correlations between neurons from aging animals

We have shown how aging can affect encoding of tone information at the single neuron level (Figs. 2-4). However, complex auditory stimuli are encoded by neural populations, and therefore we speculated that these changes at the single neuron level will also alter population activity. Pairwise neuronal signal and noise correlation are measures of functional connectivity and can reveal changing interactions between neurons (Averbeck et al., 2006; Rothschild et al., 2010; Winkowski and Kanold, 2013; Downer et al., 2017). Signal correlation measures the correlation of the average responses of two neurons to different sound stimuli and therefore reflects the tuning similarity between neurons.

In our paradigm, we presented tones in a white noise background. Because white noise contains spectral energy across all frequencies, it should drive multiple neurons and increase signal correlations between cells. As such, we predicted that the addition of white noise to a constant level tone in quiet should increase activity correlations between cells compared with presenting tones in quiet.

Indeed, this predicted pattern of pairwise signal correlation is seen in neurons from young animals (Fig. 5*A*). Signal correlation increases between the pure tone and +20 dB SNR condition and then decrease as SNR is further reduced. In aging animals, however, this pattern is disrupted, and there is no clear effect of SNR on average correlation level. Additionally, signal correlations in aging animals are significantly larger than in young animals (age × SNR ANOVA age * SNR interaction, $F_{(1,3)} = 301$, $p < 0.0001$; *post hoc* tests, tones: $p = 5.8–8$, +20 dB: $p = 5.99e\text{-}8$, +10: $p = 5.98e\text{-}8$, 0: $p = 5.98e\text{-}8$). These results were also consistent when comparing by sex (Fig. 5*B*,*C*) and when comparing results by animal (Fig. 5*D–F*). Therefore, neurons in aging animals are responding together and are tuned more similarly to each other than neurons in young animals.

We next investigated whether noise correlations are also altered in aging animals (Fig. 6). Noise correlation is defined as the remaining trial-to-trial correlation between two neurons after removing signal correlations. These correlations are important, as even weak noise correlations can have a large impact on how well neural populations can encode stimuli (Abbott and Dayan, 1999; Nirenberg and Latham, 2003), with reduced noise correlation leading to better performance (Cohen and Maunsell, 2009; Mitchell et al., 2009). We find that noise correlations are significantly larger in aging neurons than in young neurons across all sound levels (Fig. 6*A*) and for both sexes individually (Fig. 6*B*,*C*). However, when comparing the noise correlations results by animal we find that only males show a significant effect of age on noise correlation (Fig. 6*E*,*F*; age × SNR ANOVA, males: main effect of age, $F_{(1)} = 7.43$, $p = 0.0087$; females, main effect of age, $F_{(1)} = 1.01$, $p = 0.324$). Collectively, this shows that neuronal activity of A1 neurons in aging animals is more correlated to each other compared with neurons in young animals.

Both signal and noise correlations in adult animals show a dependence on the spatial distance between neurons (Winkowski and Kanold, 2013; Rupasinghe et al., 2021) likely reflecting the spatial topology of intercortica and intracortical circuits (Watkins et al., 2014; Meng et al., 2017). Therefore, we next investigated how aging altered this distance dependence of pairwise correlations (Fig. 7). We find, as expected, that pairwise signal correlations decrease as distance between neurons increases for all conditions (Fig. 7*A*). Neuronal cell pairs from aging animals also showed a distance dependence of signal correlations, but the absolute amplitude of signal correlations was higher in the pure tone condition as well as for +20 and +10 dB SNR. These data suggest that the increase in signal correlations in aging over young animals does not depend on distance between neurons and that the underlying circuits that give rise to the

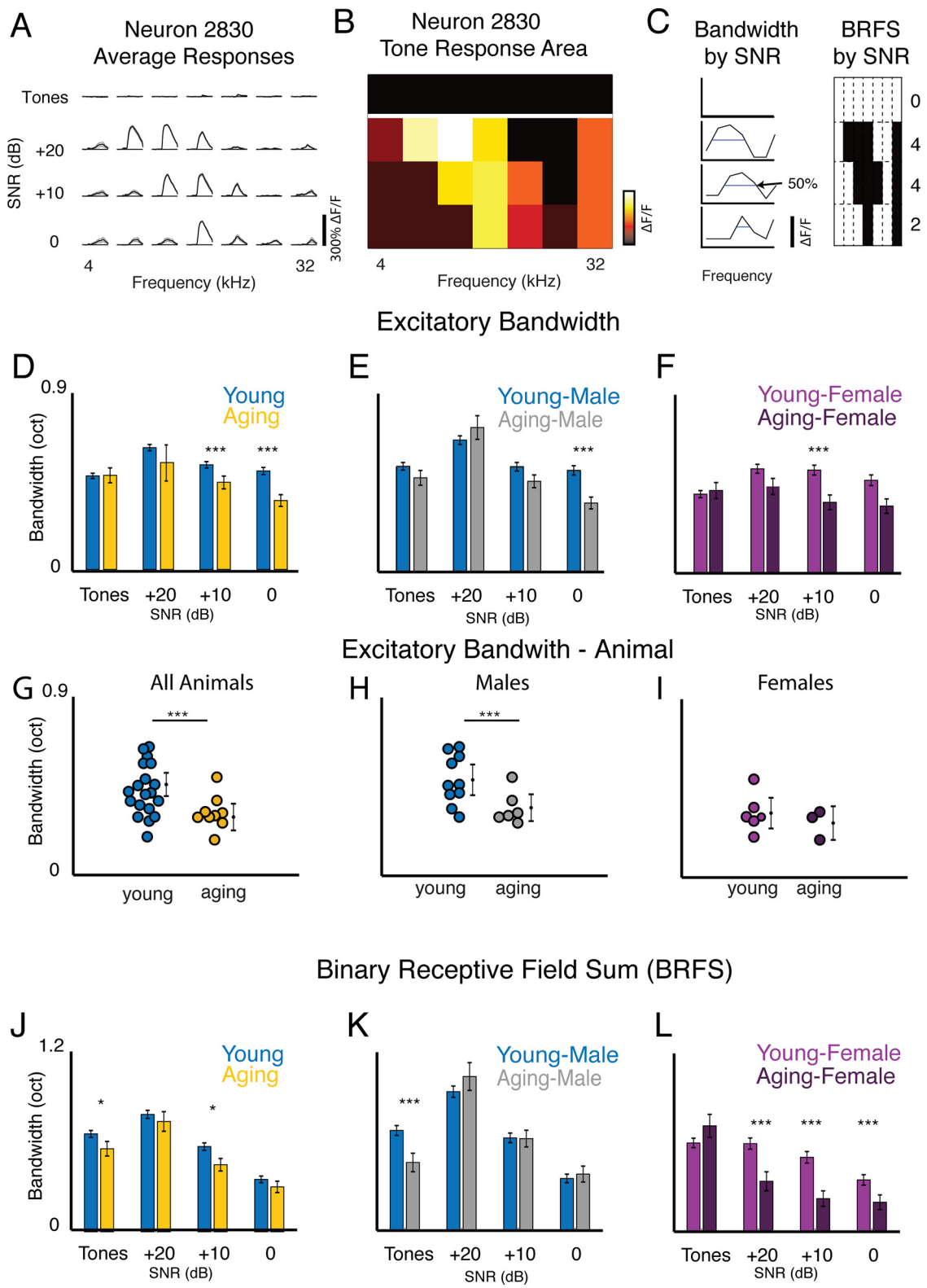

Figure 3. Aging neurons have sex-dependent change in excitatory bandwidth. ***A–C***, Cartoon illustrating calculation of bandwidth. To obtain the bandwidth at each SNR, we first obtained the average response to each stimulus. ***B***, We created a tone response plot by obtaining the average fluorescence during the tone period. ***C***, Bandwidth at each SNR is the full-width at half-maximum response. BRFS is calculated as the number of frequency bins that gave a response. ***D–F***, Excited bandwidth plotted as a function of SNR. ***D***, Comparing all young and aging animals (age × SNR ANOVA, age * SNR interaction: $F_{(1,3)} = 9.05$, $p = 5.05\text{e-}6$; *post hoc* tests, tones: $p = 0.96$, +20: $p = 0.72$, +10: $p = 0.01$, 0: 1.0e-4). ***E–F***, Comparing by sex. ***E***, Aging males (age * SNR interaction: $F_{(1,3)} = 8.12$, $p = 2.13\text{e-}5$; *post hoc* tests, tones: $p = 0.76$, +20: $p = 0.35$, +10: $p = 0.21$, 0: $p = 6.0\text{e-}4$). ***F***, Aging females (age * SNR interaction, $F_{(1,3)} = 4.03$, $p = 0.007$; *post hoc* tests, tones: $p = 0.99$, +20: $p = 0.44$, +10: $p = 0.03$, 0: $p = 0.24$). ***G–I***, Average bandwidth for each animal at each SNR. The same age × SNR ANOVA was calculated, but we only examine the main effect of age. ***G***, All aging animals (age × SNR ANOVA main effect of age, $F_{(1)} = 12.8$, $p = 5.55\text{e-}4$). ***H***, Males (age × SNR ANOVA main effect of age, $F_{(1)} = 12.06$, $p = 9.99\text{e-}4$). ***I***, Females (age × SNR ANOVA main effect of age, $F_{(1)} = 1.68$, $p = 0.21$). ***J***, Binary receptive field sum for all animals (age × SNR ANOVA age * SNR interaction, $F_{(1,3)} = 1.52$, $p = 0.207$). ***K***, BRFS males, $F_{(1,3)} = 11.5$, $p < 0.0001$; *post hoc* tests, tones: $p < 0.0001$, +20: $p = 0.1784$, +10: $p < 0.0001$, 0: $p = 0.996$. ***L***, BRFS females, $F_{(1,3)} = 15.07$ $p < 0.0001$; *post hoc* tests, tones: $p = 0.15$, +20: $p < 0.0001$, +10: $p < 0.0001$, 0: $p = 0.015$.

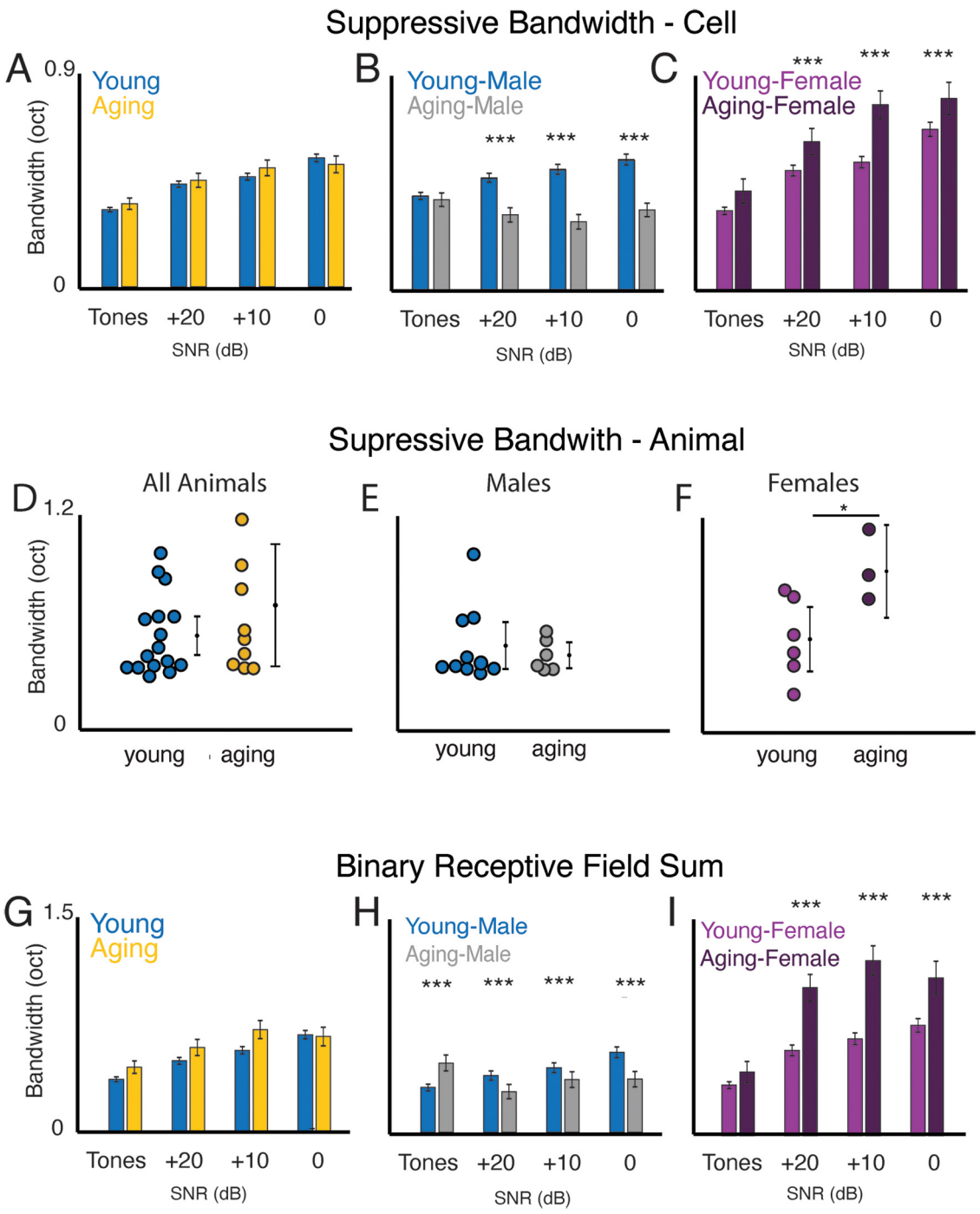

Figure 4. Aging neurons have sex-dependent change in suppressed bandwidth. ***A–F***, Analysis of suppressed responses. ***A***, Suppressed bandwidth for cells in young and aging mice (age * SNR interaction, $F_{(1,3)} = 1.60$, $p = 0.16$; *post hoc* tests, tones: $p = 0.92$, +20: $p = 0.68$, +10: $p = 0.99$, 0: $p = 0.96$). However, this changes when comparing by sex. ***B***, Suppressed bandwidth in aging males (age * SNR interaction, $F_{(1,3)} = 8.84$, $p = 7.73\text{e-}6$; *post hoc* tests, tones: $p = 0.98$, +20: $p = 1.0\text{e-}3$, +10: $p = 6.40\text{e-}8$, 0: $p = 6.20\text{e-}8$). ***C***, Suppressed bandwidth in aging females (age * SNR interaction, $F_{(1,3)} = 3.51$, $p = 0.01$; tones: $p = 0.58$, +20: $p = 0.011$, +10: $p = 5.99\text{e-}8$, 0: $p = 8.40\text{e-}3$). ***D–F***, Suppressed bandwidth by animal. ***D***, All young and aging animals (age × SNR ANOVA main effect of age, $F_{(1)} = 12.06$, $p = 9.99\text{e-}4$). ***E***, Males (age × SNR ANOVA main effect of age, $F_{(1)} = 1.07$, $p = 0.30$). ***F***, Females (age × SNR ANOVA main effect of age, $F_{(1)} = 13.02$, $p = 0.0012$). ***G***, Binary receptive field sum for all animals (age × SNR ANOVA age * SNR interaction, $F_{(1,3)} = 4.60$, $p = 0.0032$; *post hoc* tests, tones: $p = 0.109$, +20: $p = 0.053$, +10: $p = 0.001$, 0: $p = 0.998$. ***H***, BRFS males, $F_{(1,3)} = 16.9$, $p < 0.0001$; *post hoc* tests, tones: $p = 0.002$, +20: $p = 0.0584$, +10: $p = 0.35$, 0: $p < 0.0001$. ***I***, BRFS females, $F_{(1,3)} = 15.07$, $p < 0.0001$; *post hoc* tests, tones: $p = 0.624$, +20: $p < 0.0001$, +10: $p < 0.0001$, 0: $p < 0.0001$.

distance dependence seem intact. This pattern was observed in males (Fig. 7*B*), whereas in aging females (Fig. 7*C*) the distance dependence of signal correlations at 20 dB SNR seemed to be abolished. We next investigated the distance dependence of noise correlations (Fig. 7*D*). Again, in young animals we found the expected distance dependence. In contrast, noise correlations from cell pairs in aging animals showed little to no distance dependence but were always of higher magnitude. Thus, aging has a differential effect on distant cell pairs in that it increases noise correlations much more than for close-by neuronal pairs. Separating animals by sex showed similar patterns (Fig. 7*E*,*F*), with cell pairs from aging males showing consistently higher

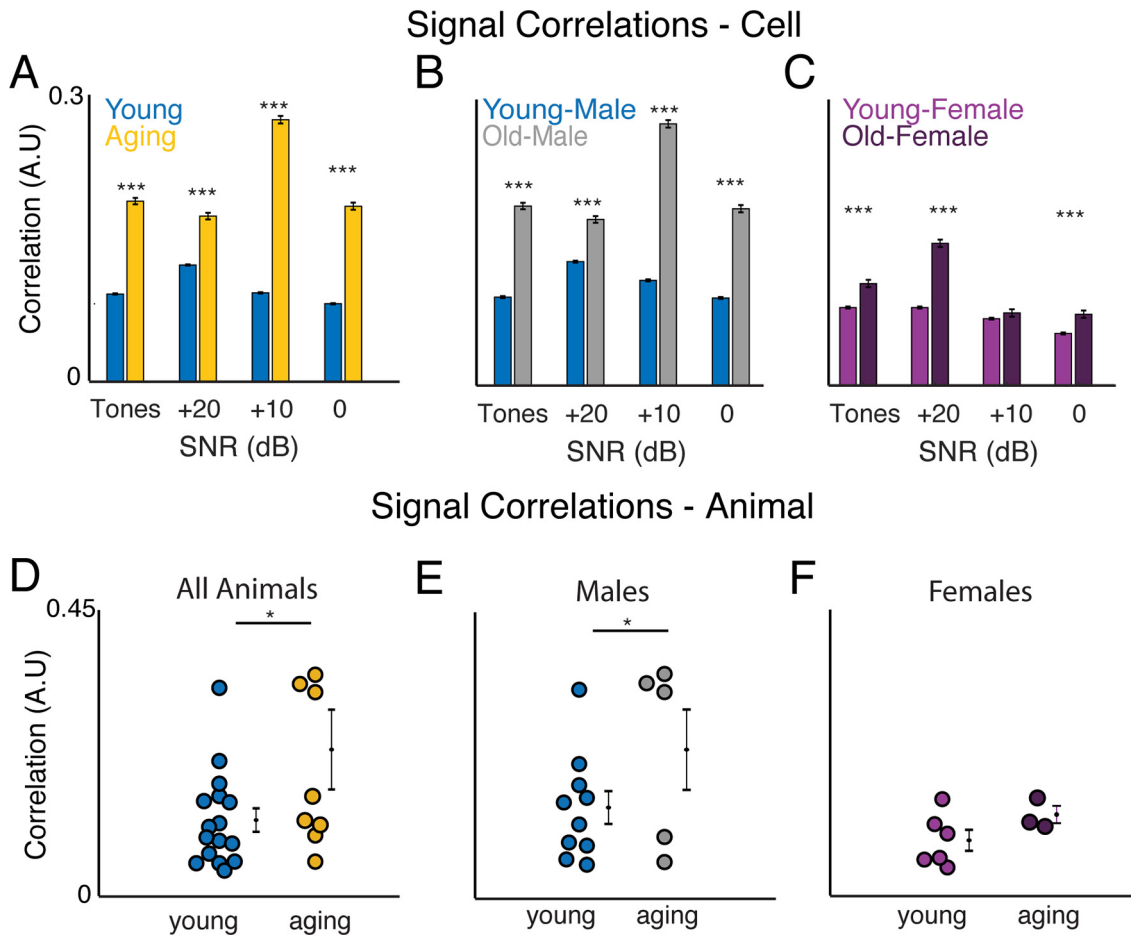

Figure 5. Aging neurons have higher signal correlations. ***A–C***, Signal correlations were calculated between each pair of neurons in an experiment for each SNR. The average correlation value ±95% CI is plotted. ***A***, Aging neurons have increased signal correlation across all SNRs (age × SNR ANOVA age * SNR interaction, $F_{(1,3)} = 303$, $p < 0.0001$; *post hoc* tests, tones: $p = 5.8\text{-}8$, +20 dB: $p = 5.99\text{e-}8$, +10: $p = 5.98\text{e-}8$, 0: $p = 5.98\text{e-}8$). ***B***, Neurons from males (age × SNR ANOVA age * SNR interaction, $F_{(1,3)} = 551$, $p< 0.0001$; *post hoc* tests, tones: $p = 5.8\text{-}8$, +20 dB: $p = 5.99\text{e-}8$, +10: $p = 5.98\text{e-}8$, 0: $p = 5.98\text{e-}8$). ***C***, Neurons from females (age × SNR ANOVA age * SNR interaction, $F_{(1,3)} = 155$, $p < 0.0001$; tones: $p = 5.8\text{-}8$, +20 dB: $p = 5.99\text{e-}8$, +10: $p = 0.42$, 0: $p = 6.15\text{e-}8$). ***D–F***, Signal correlations at the animal level. ***D***, All animals (age × SNR ANOVA, main effect of age, $F_{(1)} = 4.74$, $p = 0.032$). ***E***, Males (age × SNR ANOVA main effect of age, $F_{(1)} = 5.68$, $p = 0.027$). ***F***, Females (age × SNR ANOVA main effect of age, $F_{(1)} = 2.42$ $p = 0.12$).

noise correlations across distance than young males. In aging females, noise correlations were higher across distance for tones in quiet. However, in the tone-in-noise conditions, noise correlations were similar between young and aging animals for close-by cells and diverged for distant cell pairs. Thus, aging seems to increase noise correlations across cell pairs but has a stronger effect on distant cell pairs. Because noise correlations can be reflective of intracortical connections, this suggests that both intracortical and intercortical circuits mediating connections across 100 s of micrometers might be affected. Together, these results show that aging leads to increases in both signal and noise correlations but that there are distinct differences likely reflecting an effect of aging on separate circuits.

Aging neurons show sex-dependent loss of temporal responses

After showing that there are changes in the responses to tones, we explored whether at least some of these deficits could be explained by altered temporal response dynamics of the neurons. Neurons in A1 generally have the strongest response to large transitions in sound amplitude such as the onset or offset of a sound (Liu et al., 2019). A disruption of this temporal response pattern could impair auditory processing. For example, as we have shown that aging neurons are more excitable than younger neurons (Fig. 2), this increased excitability may cause normally tone-offset neurons to lose noise-invariant responses and also, or even exclusively, respond to noise onset.

We thus investigated the temporal response pattern of neurons and consequently of neuronal populations in each animal. To determine when each neuron had the strongest response, we analyzed the average temporal response of the neuron across all stimuli. We then identified the time point with the greatest Δ response by computing the derivative of the temporal response. For each animal we then plotted a histogram of the resulting time points at 500 ms time bins (Fig. 8*A*,*B*). We then defined significant population response bins as time bins that have a significantly higher percentage of peak responsive cells than in the prestimulus silence. All statistics shown are in comparison to the first time bin, but general significance patterns still apply if the second time bin is used for comparison. We defined onset and offset responses as the first bin after stimulus onset/offset. As expected, A1 neurons in young animals are particularly tuned to sound transitions. This is reflected in quiet by the large fraction of cells in each animal that maximally responded to tone onset and tone offset (Fig. 8*C*; ANOVA $F_{(9)} = 17.1$, p =7.8e-18; *post hoc* tests, tone onset: p = 1.26e-7, tone offset: p = 2.343-6). In noise,

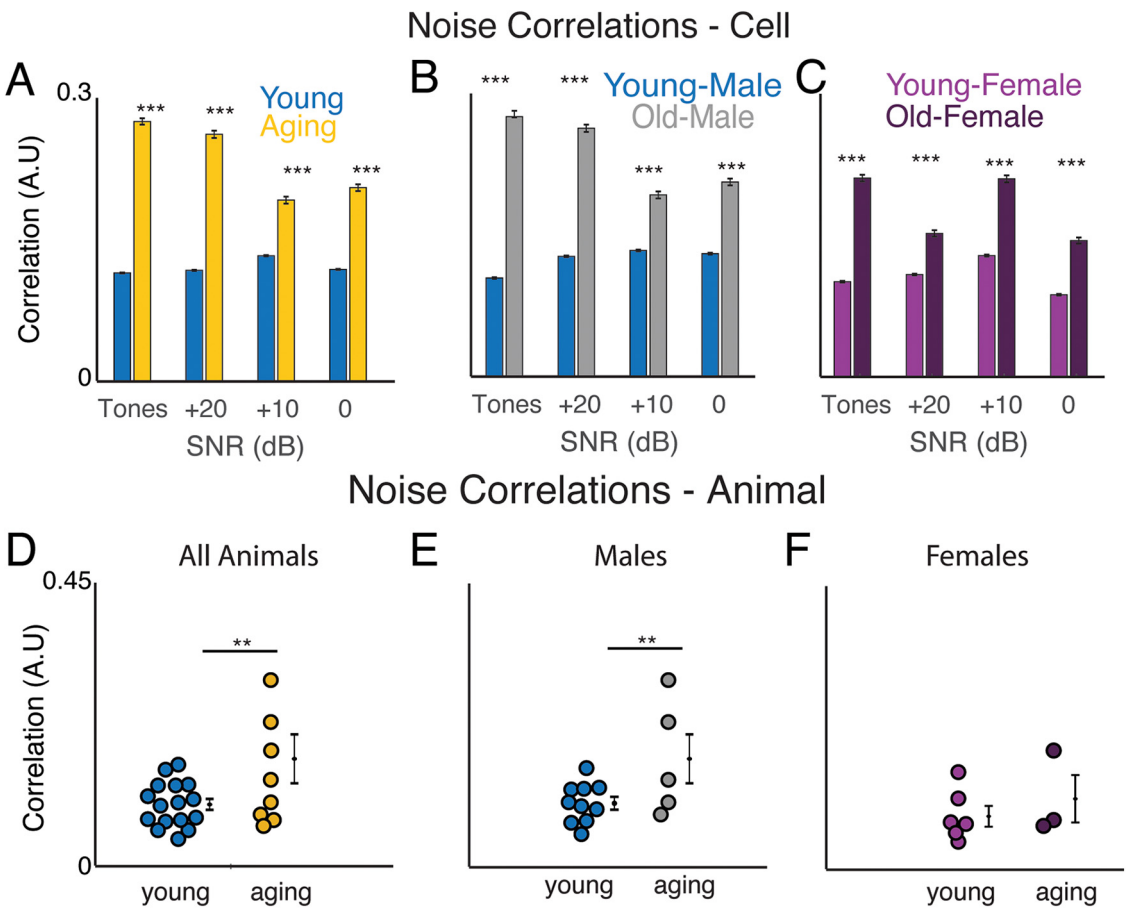

Figure 6. Aging neurons have increased noise correlation. ***A–C***, Noise correlations were calculated between each pair of neurons in an experiment for each SNR. The average correlation value ±95% CI is plotted. ***A***, Aging neurons have increased noise correlations across all SNR (age × SNR ANVOA age * SNR interaction, $F_{(1,3)} = 410$, $p < 0.001$; *post hoc* tests, tones: $p = 5.8$-8, +20 dB: $p = 5.99$e-8, +10: $p = 5.98$e-8, 0: $p = 5.98$e-8). ***B***, Neurons in males (age * SNR interaction, $F_{(1,3)} = 395$, $p < 0.0001$l; *post hoc* tests, tones: $p = 5.99$–8, +20 dB: $p = 5.99$e-8, +10: $p = 5.99$e-8, 0: $p = 5.99$e-8). ***C***, Neurons in females (age * SNR interaction, $F_{(1,3)} = 337$, $p < 0.0001$; *post hoc* tests, tones: $p = 5.99$-8, +20 dB: $p = 5.99$e-8, +10: $p = 5.99$e-8, 0: $p = 5.99$e-8). ***D–F***, Noise correlations by animal. ***D***, All animals (age × SNR ANOVA main effect of age, $F_{(1)} = 7.65$, $p = 0.007$). ***E***, Male animals (age × SNR ANOVA main effect of age, $F_{(1)} = 7.43$, $p = 0.0087$). ***F***, Females (age × SNR ANOVA main effect of age, $F_{(1)} = 1.01$, $p = 0.32$).

A1 neurons from young animals also responded maximally to noise onset and tone onset (Fig. 8*D*; ANOVA $F_{(9)} = 16.8$, $p = 1.7$-17; *post hoc* tests, noise onset: $p = 1.13$e-6, tone onset: $p = 1.27$e-7, noise offset $p = 0.045$). The percentage of neurons primarily responding to tone offset in noise was not significant ($p = 0.079$).

Neurons from aging animals showed sex-dependent changes in the pattern of temporal peak responses. In aging males, neurons predominantly showed peak responses to tone onset in quiet (Fig. 8*E*, right; ANOVA $F_{(9)} = 1.81$, $p = 0.08$; *post hoc* tests, tone onset: $p = 0.045$), and in noise they showed peak responses mostly to noise onset (Fig. 8*F*, right; ANOVA $F_{(9)} = 9.43$, $p = 1.3$e-5; *post hoc* tests, tone offset: $p = 4.34$e-5). whereas offset responses of any kind were largely absent. Thus, neurons in aging males seemed to maximally respond to any sound onset transition. Aging females had the opposite phenotype and were biased to maximally respond to tone or noise offsets (Fig. 8*G*,*H*, right). In quiet, cells from females showed maximal responses to tone offset (Fig. 8*G*, right; ANOVA $F_{(9)} = 9.43$, $p = 1.3$e-5; *post hoc* tests, tone offset: $p = 4.34$e-5), and in noise they showed maximal responses to tone onset and tone offset with a higher fraction of neurons responding to tone offset (Fig. 8*H*, right; ANOVA $F_{(9)} = 16.36$, $p = 2.17$e-7; *post hoc* tests, tone onset: $p = 0.012$, noise offset: $p = 6.67$e-6), noise offset: $p = 6.70$e-7). These data suggest that one consequence of aging is a loss of temporal response diversity.

Aging neurons show loss of temporal response diversity in a sex-dependent manner

A1 neurons are diverse with respect to spectrotemporal receptive fields and temporal responses (Sutter and Schreiner, 1991; Francis et al., 2018; Liu et al., 2019; Liu and Kanold, 2021). *In vitro* circuit analysis suggested that the functional diversity of A1 L2/3 responses could be caused by different classes of cells with different connection properties (Meng et al., 2017). Thus, given the altered spectrotemporal sensitivity in aging, we reasoned that this reduction could be the result of a reduction of the diversity of responses in the neural population.

We compared the diversity of functional responses between groups by clustering the neurons of both young and aging mice into clusters with distinct patterns of stimulus-driven activity using K-means clustering (Fig. 9*A–C*). Neurons formed nine total clusters based on the average response of each neuron to the tone-in-noise stimulus (Fig. 9*B*) but not all clusters were present in all animals (Fig. 9*C*) as detailed below. The clusters varied in temporal responses and could be further grouped by dominant stimulus-driven responses into excited (Fig. 9*D*), suppressed (Fig. 9*E*), and mixed responses (Fig. 9*F*). Each plot in Figure 9, *D–F*, shows the characteristic response profile of that cluster. The cluster proportions of the young animals split evenly between clusters (Fig. 9*B*). The two largest excited clusters for young animals (cluster 2–3) both have negligible noise responses

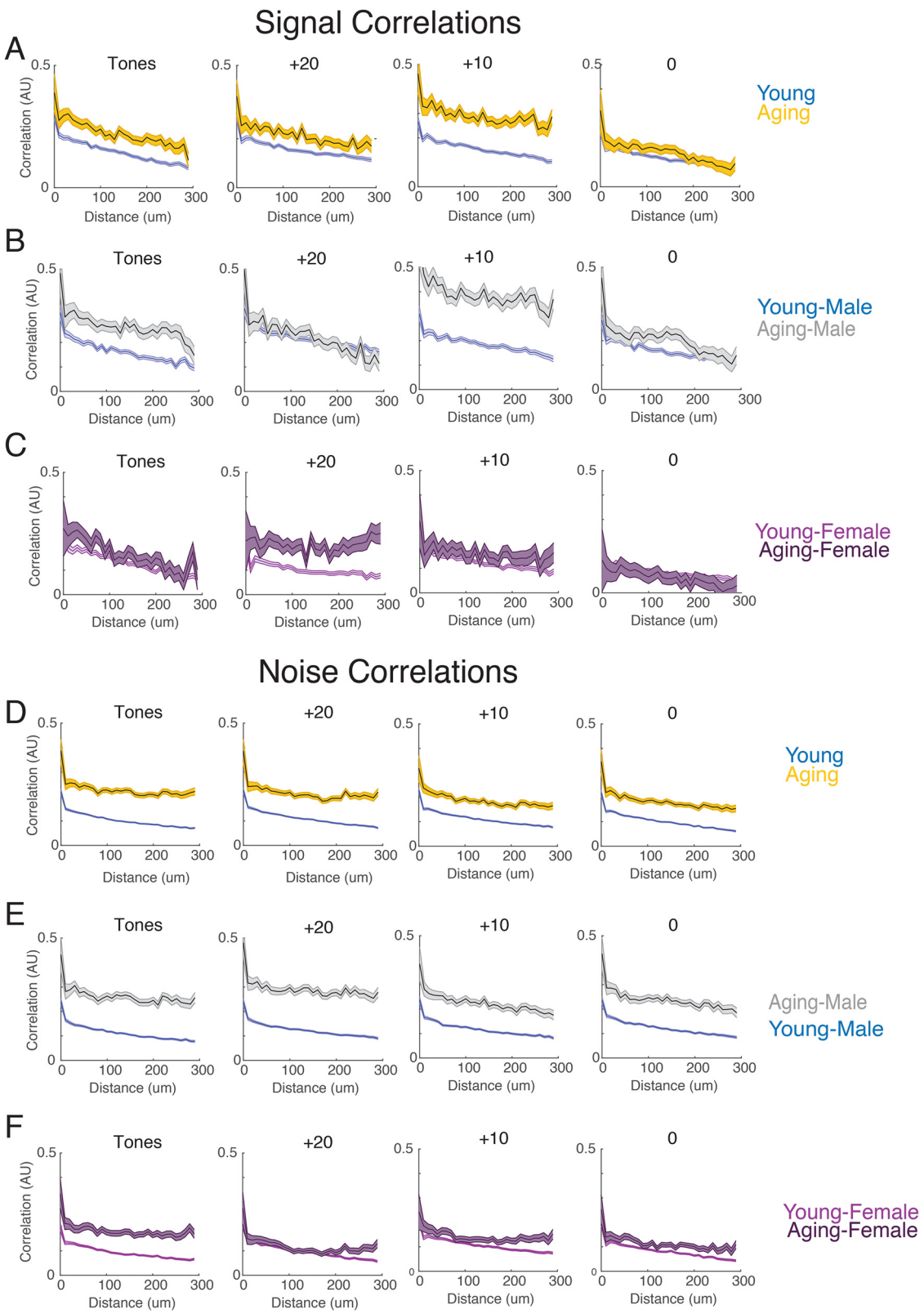

Figure 7. Distance dependence of pairwise correlations changes with aging. ***A–C***, Signal correlations from pairs of neurons in young and aging animals as function of distance (10 μm bins). All error bars indicate 95% confidence intervals. Signal correlations of young and aging animals (***A***). Comparison of sex, signal correlations of comparing young and aging (***B***) male and (***C***) female animals. ***D–F***, Noise correlations from pairs of neurons in young and aging animals as function of distance. Noise correlations between young and aging animals (***D***). Comparison of sex, noise correlations of comparing young and aging (***E***) male and (***F***) female animals.

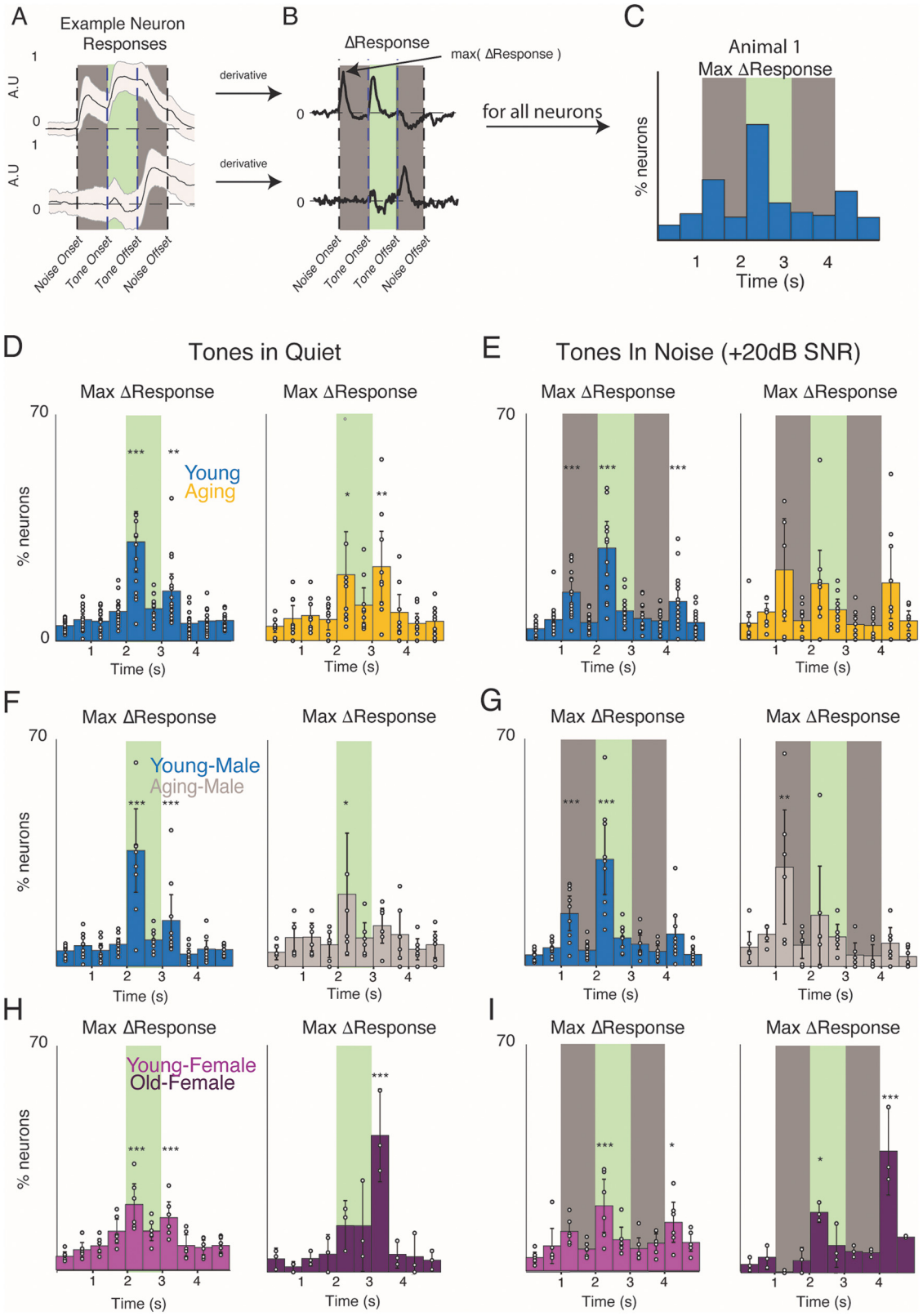

Figure 8. Aging neurons have altered temporal responses. ***A***, Example neuronal responses to tone-in-noise stimuli. Green bars indicate the period when the tone stimulus was presented. Gray bars indicate when noise was presented. Note that noise duration includes tone presentation period. ***B***, To calculate the Δ response of each neuron, the derivative of ***A*** is taken, and the time point with the largest change in response magnitude is determined. Resulting peak time points are binned to create histograms. ***C–H***, Bins were considered significantly peak responding if they had a significantly larger proportion of cells responding than the prestimulus silence period, which corresponds to the first two time bins. ***C***, In quiet, young neurons significantly respond to tone onset and offset (age × time ANOVA age * time interaction, $F_{(1,9)} = 17.1$, $p = 7.8e\text{-}18$; *post hoc* tests, tone onset: $p = 1.26e\text{-}7$, tone offset: $p = 2.343e\text{-}6$), as do aging neurons (age × time ANOVA age * time interaction, $F_{(1,9)} = 3.81$, $p = 4.78e\text{-}8$; *post hoc* tests, tone onset: $p = 0.03$, tone offset $p = 0.005$). ***D***, In noise, young neurons significantly responded to noise onset, tone onset, and tone offset (age × time ANOVA age * time interaction, $F_{(1,9)} = 16.8$, $p = 1.7–17$; *post hoc* tests, noise onset: $p = 1.13e\text{-}6$, tone onset: $p = 1.27e\text{-}7$, noise offset $p = 0.045$). ***E–H***, Analysis by sex. Aging males (***E***, ***F***)

and have a large tone response, indicating they encode tones in a noise-invariant manner.

In contrast, neurons in aging animals are concentrated in only 5 five clusters, with one cluster accounting for 45% of all neuronal responses (Fig. 9*B*). Notably, this main cluster for aging animals (cluster 1) preferentially responds to noise over tones, consistent with our earlier findings. The two clusters that have noise-invariant responses (clusters 2–3) are also reduced. Aging animals additionally have a loss of suppressed responses, as <5% of all neurons recorded from aging animals were in a suppressed category (clusters 4–6). Instead, there seems to be an increase in neurons with a very slow temporal response (cluster 9).

To quantitatively determine how the diversity of response clusters change with age, we calculated the number active clusters in each animal (Fig. 9*C*). We defined active clusters as those with at least 5% of the neural representation in the field of view. Averaging over experiments, we found a significant reduction in cluster diversity in the aging animal (Fig. 9*C*; Student's *t* test, $t = 2.40$, $p = 0.021$). Separating these results by sex, we found that this result only holds for the male mice (Fig. 9*C*; Student's *t* test, males: $t = 2.18$, $p = 0.049$, females $t = 1.43$, $p = 0.197$). These results indicate a reduction of population diversity in aging male mice and, in particular, a loss of cells with suppressed and dynamic responses in aging A1.

To quantify which classes of activity were lost in males and females, we separated our results from Figure 9 by sex and analyzed cluster diversity (Fig. 10*A–D*). We find that aging females (Fig. 10*A*), have primarily lost excited classes of responses. However, the few excited responses they do have belong to the class of excited neurons that is more robust to noise (Fig. 10*B*, cluster 1). Aging male animals, on the other hand (Fig. 10*C*,*D*), have primarily lost suppressed clusters. A majority of aging male neurons belong to two classes of excited responses that have a large response to noise (Fig. 10*C*, clusters 2, 4; 80% of total neurons). These data indicate a sex-dependent loss of classes of neural activity.

Young neurons encode tone information better than aging neurons

Our data show there are increased correlations and reduced sensitivity to tone onset and offset in the A1 of aging animals. Onset and offset responses are thought to be the basis for sound source separation (Bregman, 1990). The loss of these responses will impair accurate detection of the tone in noise. Neuronal correlations can also affect coding of information (Averbeck et al., 2006). We thus predict that these changes in neuronal activity with age will have an impact on neuronal signal detection in the aging A1. To test this hypothesis, we trained a naive Bayes decoder model (Maron, 1961; Fig. 11*A*) on the neural responses of young and aging mice to decode the tone played during each trial. For each model, we ran a 10-fold cross-validated model on a randomly selected subpopulation of neurons to prevent overfitting. We then ran 10 such models with a new selection of neurons and plotted the average model accuracy and 95% confidence intervals (Fig. 11*B*). We varied the numbers of neurons included to identify whether additional neurons increased classification accuracy. Classification accuracy increased as a function of the number of neurons added to the classifier for both young and aging neurons. However, models trained on neurons from the young animal group obtained significantly better decoding accuracy as the number of neurons in the model increased (Fig. 11*A*; age × neuron ANOVA age * neuron interaction, $F_{(1,99)} = 7.75$, $p < 0.001$). Plotting the results from $n = 80$ neurons over time showed that both classifiers have chance decoding accuracy before the tone presentation (Fig. 11*C*). Chance accuracy is defined as the accuracy of randomly guessing with a uniform policy, which would give an expected mean accuracy of one/the number of tones = 1/7 or ~14%. This indicated that our results were not a consequence of overfitting. Critically, both classifiers increase accuracy during tone presentation, with the highest accuracy occurring at tone offset (Fig. 11*C*). When comparing the effect of SNR on these classifiers, we found that although these classifiers perform similarly well in quiet, the classifier trained on aging neurons performs significantly worse in noise (Fig. 11*D*; age × SNR ANOVA age * SNR interaction, $F_{(1,3)} = 34.1$, $p < 0.0001$; *post hoc* tests, tones: $p = 0.343$, +20: $p = 5.988\text{e-}8$, +10: $p = 5.8\text{e-}8$, 0: $p = 9.2\text{e-}8$). These results were also consistent for both sexes (Fig. 11*E–J*). Together, these results show that the spectral and temporal changes seen in aging A1 neurons cause impairments in encoding tones in noise.

Discussion

Our results show that mouse A1 L2/3 excitatory neurons have diverse patterns of neural activity in response to a complex tone-in-noise stimulus, with different subpopulations of neurons preferentially responding to different segments of the auditory stimulus. We also found that aging reduces the diversity of tuning to the auditory stimulus both on the single neuron and population levels. Finally, we showed with a Bayesian neural decoder that this loss in neural diversity translates to a loss in tone information especially in noisy backgrounds.

Similar to prior studies in young adult mice, we found a population of neurons in A1 that encodes sounds in a noise-invariant manner (Fig. 9*D*, clusters 2–3; Rabinowitz et al., 2013; Schneider and Woolley, 2013; Teschner et al., 2016; Christison-Lagay et al., 2017). Other studies have also found populations of neurons that primarily respond to the background sound (Las et al., 2005; Bar-Yosef and Nelken, 2007), even when that sound is much weaker in intensity. We find that these tone-invariant responses are largely lost in the aging animal (Figs. 7-9) and that instead aging neurons respond to the first change in the sound level (Fig. 10).

Our results show a lack of offset responses in A1 of aging animals to either the tone or the noise. Offset responses are a fundamental feature of auditory signal processing in A1 (He et al., 2001; Fishman and Steinschneider, 2009; Scholl et al., 2010; Baba et al., 2016; Liu et al., 2019) and are thought to be a critical component for auditory scene analysis (Bregman, 1994). The relative disappearance of offset responses in aging animals is a novel finding and likely contributes to the lack of tone information found in A1 of aging animals. This could also be a potential mechanism to understand why older adults exhibit good hearing in quiet but an inability to discriminate speech in noise (Dubno et al., 1984; Working Group on Speech Understanding and Aging, Committee on Hearing, Bioacoustics, and Biomechanics

←

only respond to sound onsets. ***E***, In quiet, they only significantly responded to tone onset (age × time ANOVA age * time interaction, $F_{(1,9)} = 1.81$, $p = 0.08$; *post hoc* tests, tone onset: $p = 0.045$) and in noise (***F***) respond to noise onset (age × time ANOVA age * time interaction, $F_{(1,9)} = 4.12$, $p = 0.003$). ***G***, ***H***, Aging females are biased to offset responses. ***G***, In quiet, they significantly respond to tone offset (age × time ANOVA age * time interaction, $F_{(1,9)} = 9.43$, $p = 1.3\text{e-}5$; *post hoc* tests, tone-offset: $p = 4.34\text{e-}5$). ***H***, In noise, they respond to tone onset and noise offset (age × time ANOVA age * time interaction, $F_{(1,9)} = 16.36$, $p = 2.17\text{e-}7$; *post hoc* tests, tone onset: $p = 0.012$, noise offset: $p = 6.67\text{e-}6$).

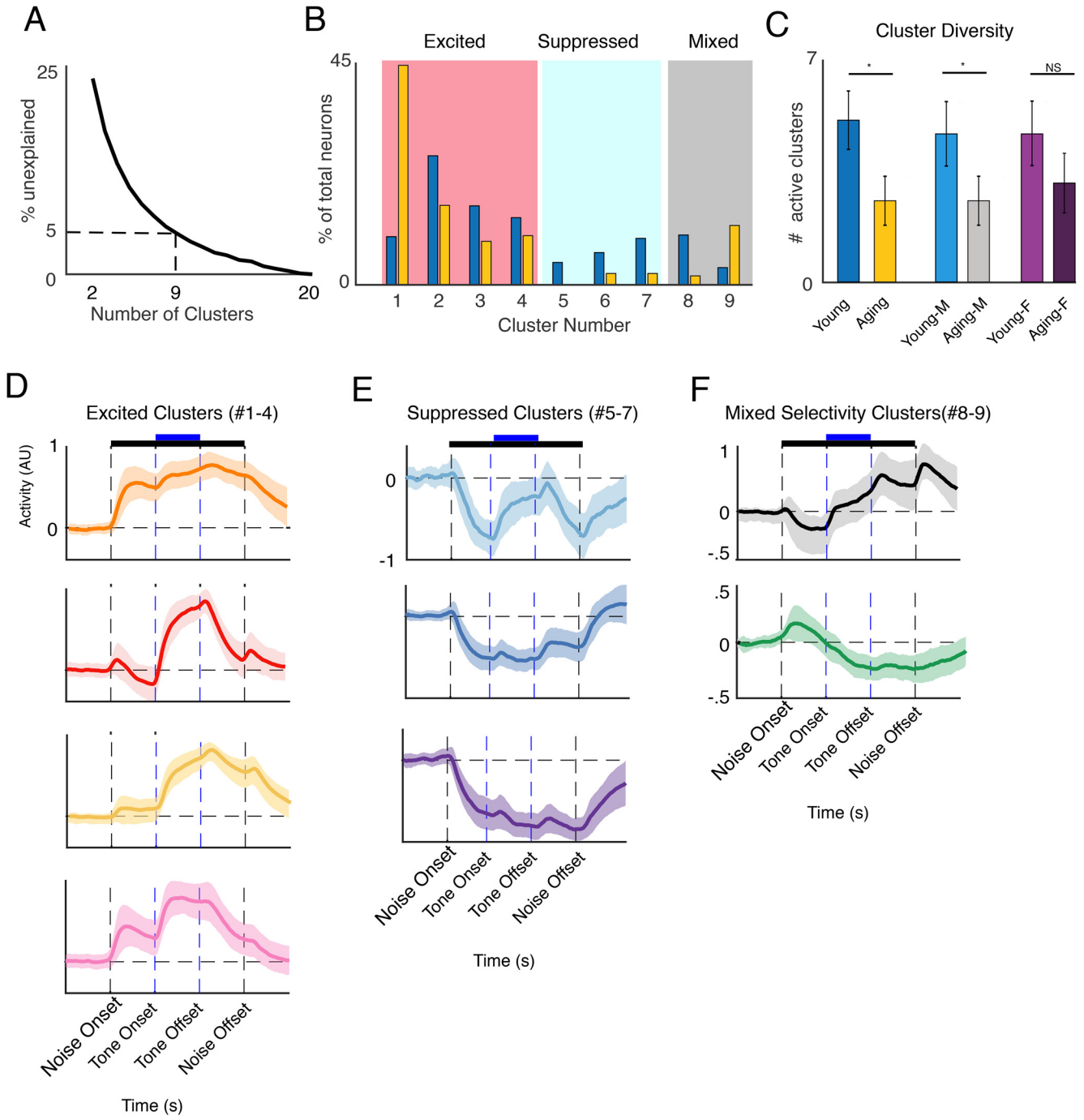

Figure 9. Aging neurons have reduced response diversity. ***A***, K-means clustering of the normalized responses of neurons to determine functional classes of neurons. Elbow criterion is used to determine the number of clusters that explain 95% of variance. This happened at nine clusters. ***B***, Cluster distribution in both groups. Bars indicate the percentage of the total population of aging or young neurons that belong to that cluster. Bars are sorted into three general categories of responses, excited, suppressed, or mixed, based on the dominant activity of the cluster. ***C***, To calculate neural response diversity, we calculated mean number of active clusters in each experiment across animals. A cluster was deemed to be active if at least 5% of neurons in the field of view belonged to that cluster. Response diversity significantly decreases in aging animals (Student's *t* test, $t = 2.48$, $p = 0.21$). Effect is only seen in aging male animals (Student's *t* aging males: $t = 2.18$, $p = 0.49$; aging females: $t = 1.43$, $p = 0.197$). ***D–F***, Average cluster response is presented for the excited, suppressed, and mixed clusters. Shaded bars indicate 95% confidence intervals.

(1988); Fitzgibbons and Gordon-Salant, 1996; Gordon-Salant and Fitzgibbons, 1995, 1999; Lister et al., 2002; Lee, 2015). Offset-responses are thought to originate in a nonlemniscal pathway to A1 (Liu et al., 2019). Thus, based on our results we speculate that this pathway may be particularly sensitive to the potential neurodegenerative effects of healthy aging.

The inability to separate signal from noise is a significant problem in aging. Similar to previous studies (Willott et al., 1988, 1993; Krukowski and Miller, 2001; Bao et al., 2004), we have shown that aging neurons exhibit more temporally and spectrally homogenous responses. One potential mechanism for these changes is that they are the result of reduced inhibition that occurs during normal aging (Caspary et al., 2008; Llano et al., 2012; Ouellet and de Villers-Sidani, 2014; Brewton et al., 2016; Cisneros-Franco et al., 2018). Our findings are consistent with this hypothesis, as we found that there are fewer suppressed

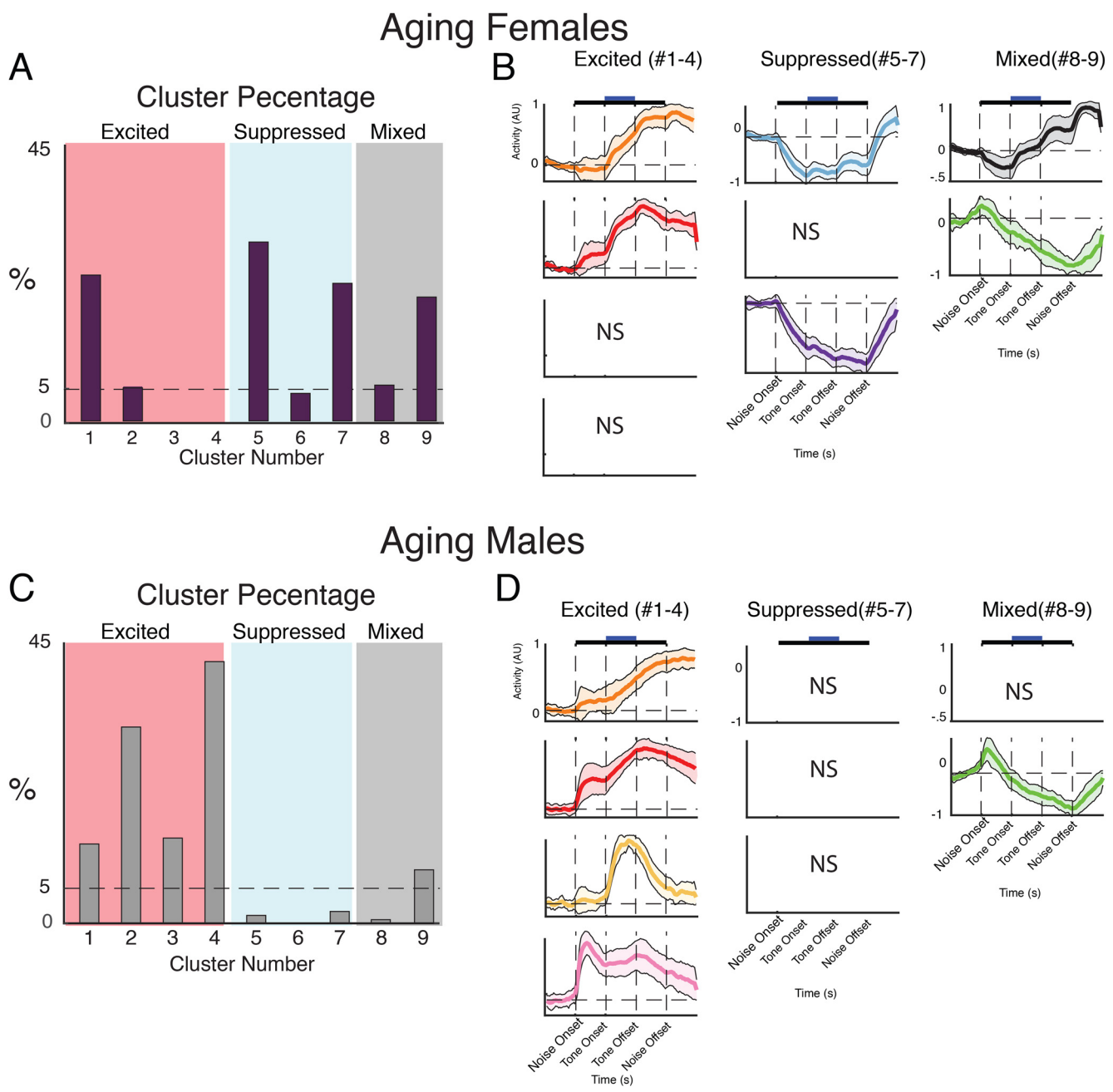

Figure 10. Aging male and female animals show different patterns of cluster loss. To visualize the clusters of neuronal responses that were still present in aging males/female, we plotted each cluster that had a least 5% of neuronal representation. ***A***, Aging females primarily had a loss excited clusters. ***B***, Visualization of the average response each cluster in ***A***. ***C***, Aging males, however, primarily show a reduction in suppressed clusters. ***D***, visualization of the average response of each cluster in ***B***.

responses, a proxy for inhibitory drive, in aging neurons as well as having a larger overall response to sound consistent with prior results (Hughes et al., 2010). This decreased suppression could be because of a reduced efficacy of inhibitory connections or a reduced number of connections, or both. There is evidence that parvalbumin-positive inhibitory neurons, which are important for stimulus selectivity, are reduced in both number and activity in aging animals (Martin del Campo et al., 2012; Cisneros-Franco et al., 2018). There is similar evidence of reduced GABAergic activity in a humans (Gao et al., 2015) and nonhuman primates (Leventhal et al., 2003). We also find that the excitatory bandwidth of neurons under certain SNRs and in our BRFSs measure decreases, consistent with prior work (Gourévitch and Edeline, 2011; Occelli et al., 2019). Although there were difference between sexes, this suggests a reduction of ascending inputs to L2/3.

Consistent with previous work (Cohen and Kohn, 2011; Winkowski and Kanold, 2013; Rupasinghe et al., 2021), we found that noise correlations were small and positive in A1 and distance dependent. We show that functional network properties are fundamentally altered by aging. Specifically, aging animals have higher noise correlations, regardless of SNR and across large distances with an increasing effect size with distance. The seemingly widespread increase in correlations in aging A1 suggests that affected circuits are also likely somewhat dispersed and might include neuromodulatory or top-down inputs (Kilgard and Merzenich, 1998; Bao et al., 2001; Winkowski et al., 2013, 2018; Caras and Sanes, 2017), possibly acting on coupled

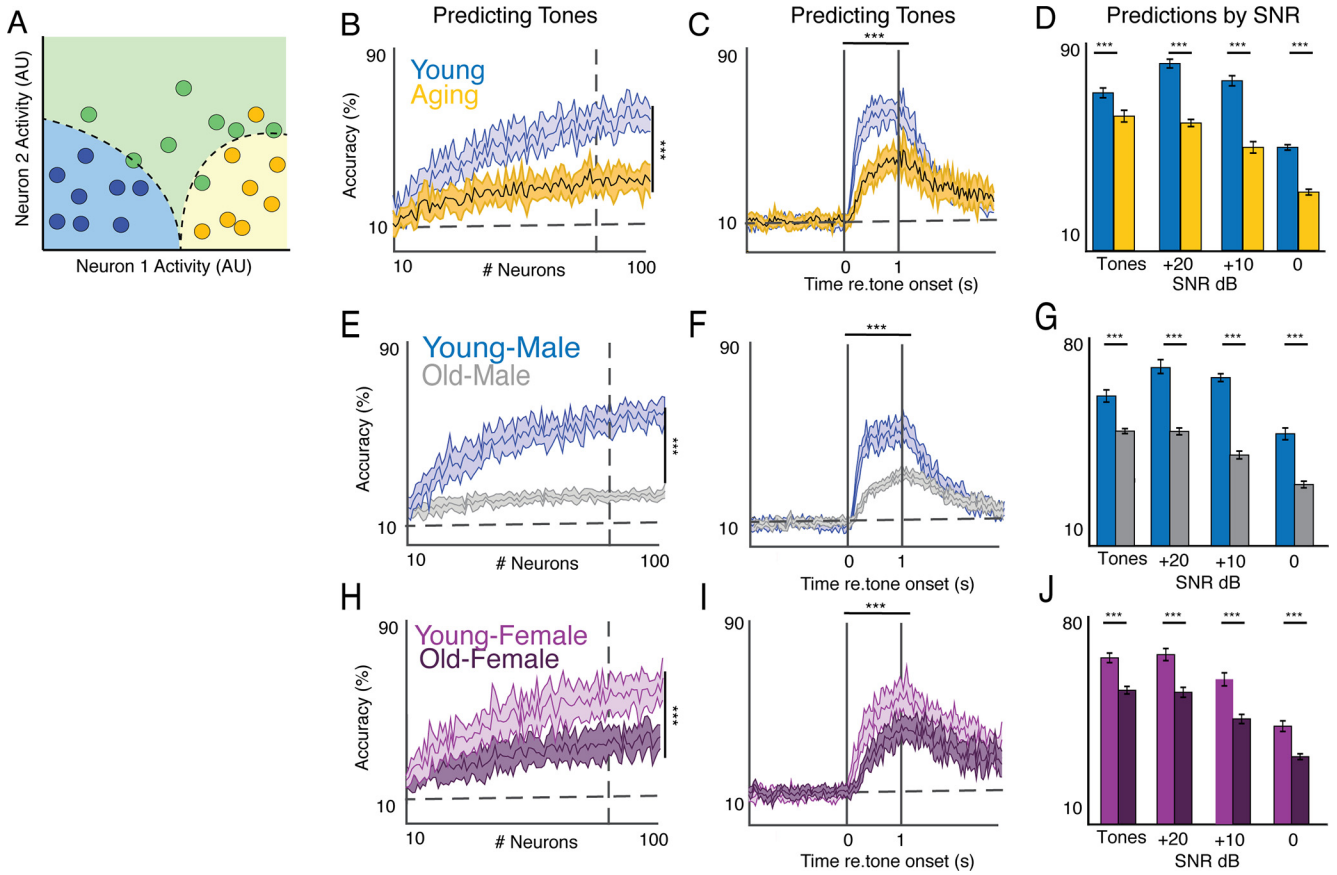

Figure 11. Aging neurons less able to discriminate between tones in noise. ***A***, Ideal observer analysis. Diagram of a naive Bayes encoder trained on two neurons to discriminate among three categories (blue, green, and yellow). Based on the labeled training data (colored circles) of how the two neurons respond for each trial, the encoder can create boundaries (dotted lines) to predict future trials. We trained naive Bayes classifier to decode tone frequency from neural activity. ***B***, Classifier accuracy improves as we include more neurons to our decoding model for both groups. In the young group, asymptotic performance was reached at ~60–70% accuracy at 80 neurons. The aging group showed little improvement between the 10- and 100-neuron model, with asymptotic performance at 34% accuracy, which is still significantly above chance (random = one-seventh chance or ~14%) Thus, the decoder trained on young animals performed significantly better (age × neuron ANOVA age * neuron interaction, $F_{(1,99)} = 7.75$, $p < 0.001$). ***C***, Using a model trained on $n = 80$ neurons, we next investigated how the accuracy of this decoder changed over the course of the stimulus presentation. Before tone onset, both models performs at chance level, indicating the models are well calibrated. Once tone onset occurs, both models increase in accuracy above chance and performance increases until tone offset. ***D***, Bar plots show the effect of SNR on detection accuracy of the models. Both models perform statistically similarly when tones are played in quiet. When noise is added, the model trained on young group data performs significantly better at the +20, +10, and +0 dB SNR conditions (age × SNR ANOVA age * SNR interaction, $F_{(1,3)} = 34.1$, $p < 0.0001$; *post hoc* tests, tones: $p = 0.343$, +20: $p = 5.988e\text{-}8$, +10: $p = 5.8e\text{-}8$, 0: $p = 9.2e\text{-}8$). ***E–G***, Comparison of young and aging males. ***E***, Performance as function of number of neurons in the model (age × neuron ANOVA, $F_{(1,99)} = 10.5$ $p < 0.0001$). ***F***, Performance as function of time (age × time ANOVA, $F_{(1,151)} = 8.98$, $p = 3.2e\text{-}47$). ***G***, Performance as function of noise levels (age × time ANOVA, $F_{(1,3)} = 23.08$, $p < 0.0001$; *post hoc* tests, tones: $p = 5.99e\text{-}8$, +20: $p = 5.99e\text{-}8$, +10: $p = 5.89e\text{-}8$, 0: $p = 5.89e\text{-}8$). ***H–L***, Comparison of young and aging females. ***H***, Performance as function of number of neurons in the model (ANOVA, $F = 787$, $p = 2.0e\text{-}146$). ***I***, Performance as function of time ($F_{(1,151)} = 8.98$, $p < 0.0001$). ***J***, Performance as function of noise levels (age × SNR ANOVA age * SNR interaction, $F_{(1,3)} = 323$, $p < 0.0001$; *post hoc* tests, tones: $p = 5.89e\text{-}8$, +20: $p = 5.89e\text{-}8$, +10: $p = 5.89e\text{-}8$, 0: $p = 5.99e\text{-}8$).

inhibitory networks (Postma et al., 2011; Kraft et al., 2020). The distinct differences in the distance dependence of signal and noise correlations in aging suggests that multiple distinct circuits are affected.

Altered pairwise correlations have functional consequences. Multiple studies have suggested that reduced noise correlations improve decoding accuracy (Cohen and Maunsell, 2009, 2010; Renart et al., 2010; Cohen and Kohn, 2011; Mendels and Shamir, 2018). This suggests that increased noise correlations in aging A1 is one potential mechanism for decreased speech intelligibility in noise for subjects with impaired hearing.

A1 layer 2/3 responses are functionally heterogeneous, emerging from different excitatory and inhibitory connection patterns (Meng et al., 2017). For example, in auditory cortex, Malone et al. (2017) have shown at least three different classes of neuronal responses to tones in noise. Auditory cortex has higher heterogeneity and lower noise correlation than more peripheral auditory stations (Rabinowitz et al., 2013). Theoretical approaches have posited that larger functional diversity can improve sensory encoding (Ecker et al., 2011; Tripathy et al., 2013) and that this diversity is particularly important for temporal encoding (Perez-Nieves et al., 2020). Therefore, this work suggests that central auditory circuits are degraded during aging, leading to the loss of neuronal heterogeneity and increased noise correlation, and that these changes lead to poor stimulus encoding.

The data presented here support this interpretation. Our clustering results show that the loss of suppressed activity leads to a loss of response heterogeneity in L2/3 neurons. Aging neurons become noise responsive (matching the temporal data in Fig. 8). This increase in homogeneity would also lead to the increased activity correlations (Figs. 5, 6). Finally, this also explains the decoding results (Fig. 11), as the majority of neurons in aging mice belong to clusters with little or no tone response (Fig. 7*B*, clusters 1, 9). These results support the emerging literature regarding the importance of response diversity to sensory

encoding (Holmstrom et al., 2010; Tripathy et al., 2013; Kastner et al., 2015; Berry et al., 2019).

Our data also uncovered a significant effect of sex. Aging males were more correlated (Figs. 5-7), had larger reduction in response diversity (Figs. 8, 9), and consequently had worse performance in neural decoding than aging females (Fig. 11). Additionally, on several measures such as bandwidth (Figs. 3, 4), correlations (Figs. 5-7), and clustering (Fig. 10), aging male and female animals had different or even opposite results, suggesting that the aging process affects male and female A1 differently. We believe that this unexpected and important finding suggests that more work needs to be done to investigate whether this extends to humans, especially on behavioral measures.

Disentangling the central effects of hearing loss from peripheral effects is challenging. To mitigate peripheral effects, we used several methods. We used a mouse model known to have good hearing and genotyped all mice to ensure they did not carry an early hearing loss genotype. As hearing loss can change cortical map plasticity (Willott et al., 1993), we ensured that all animals tested showed no such reorganization and had good hearing for the range of frequencies tested (Fig. 1).

We have shown that aging affects the ability for A1 L2/3 neurons to encode tones in noise. However, as the mice tested were passively listening to the stimuli, we do not know how these neuronal responses might change under behavioral conditions. A1 responses can be shaped by attention and prefrontal inputs (Fritz et al., 2007; David et al., 2012; Winkowski et al., 2013, 2018; Francis et al., 2018, 2021). Thus, any additional attentional deficits that occur with aging could make behavioral differences even larger (Darowski et al., 2008; Basak and Verhaeghen, 2011; Golob and Mock, 2019).

Our results show that ACtx contains different populations of excitatory neurons that encode different sound features and that aging independent of peripheral hearing loss causes a loss of population response diversity, resulting in sound-encoding deficits in noisy backgrounds. Future work determining the identities of these circuits could provide new targets for future pharmacological or other interventions to improve auditory function in aging patients.

References

Abbott LF, Dayan P (1999) The effect of correlated variability on the accuracy of a population code. Neural Comput 11:91–101.

Averbeck BB, Latham PE, Pouget A (2006) Neural correlations, population coding and computation. Nat Rev Neurosci 7:358–366.

Baba H, Tsukano H, Hishida R, Takahashi K, Horii A, Takahashi S, Shibuki K (2016) Auditory cortical field coding long-lasting tonal offsets in mice. Sci Rep 6:34421.

Bandyopadhyay S, Shamma SA, Kanold PO (2010) Dichotomy of functional organization in the mouse auditory cortex. Nat Neurosci 13:361–368.

Bao S, Chan VT, Merzenich MM (2001) Cortical remodelling induced by activity of ventral tegmental dopamine neurons. Nature 412:79–83.

Bao S, Chang EF, Woods J, Merzenich MM (2004) Temporal plasticity in the primary auditory cortex induced by operant perceptual learning. Nat Neurosci 7:974–981.

Bar-Yosef O, Nelken I (2007) The effects of background noise on the neural responses to natural sounds in cat primary auditory cortex. Front Comput Neurosci 1:3.

Basak C, Verhaeghen P (2011) Aging and switching the focus of attention in working memory: age differences in item availability but not in item accessibility. J Gerontol B Psychol Sci Soc Sci 66:519–526.

Berry MJ II, Lebois F, Ziskind A, da Silveira RA (2019) Functional diversity in the retina improves the population code. Neural Comput 31:270–311.

Bowen Z, Winkowski DE, Kanold PO (2020) Functional organization of mouse primary auditory cortex in adult C57BL/6 and F1 (CBAxC57) mice. Sci Rep 10:article 10905.

Bregman AS (1990) Auditory scene analysis: the perceptual organization of sound. Cambridge, Mass: MIT.

Bregman AS (1994) Auditory scene analysis: the perceptual organization of sound. Cambridge, Mass: MIT.

Brewton DH, Kokash J, Jimenez O, Pena ER, Razak KA (2016) Age-related deterioration of perineuronal nets in the primary auditory cortex of mice. Front Aging Neurosci 8:270.

Burianova J, Ouda L, Profant O, Syka J (2009) Age-related changes in GAD levels in the central auditory system of the rat. Exp Gerontol 44:161–169.

Caras ML, Sanes DH (2017) Top-down modulation of sensory cortex gates perceptual learning. Proc Natl Acad Sci U S A 114:9972–9977.

Caspary DM, Ling L, Turner JG, Hughes LF (2008) Inhibitory neurotransmission, plasticity and aging in the mammalian central auditory system. J Exp Biol 211:1781–1791.

Chaudhry FA, Reimer RJ, Bellocchio EE, Danbolt NC, Osen KK, Edwards RH, Storm-Mathisen J (1998) The vesicular GABA transporter, VGAT, localizes to synaptic vesicles in sets of glycinergic as well as GABAergic neurons. J Neurosci 18:9733–9750.

Chen T-W, Wardill TJ, Sun Y, Pulver SR, Renninger SL, Baohan A, Schreiter ER, Kerr RA, Orger MB, Jayaraman V, Looger LL, Svoboda K, Kim DS (2013) Ultrasensitive fluorescent proteins for imaging neuronal activity. Nature 499:295–300.

Christison-Lagay KL, Bennur S, Cohen YE (2017) Contribution of spiking activity in the primary auditory cortex to detection in noise. J Neurophysiol 118:3118–3131.

Cisneros-Franco JM, Ouellet L, Kamal B, de Villers-Sidani E (2018) A Brain without brakes: reduced inhibition is associated with enhanced but dysregulated plasticity in the aged rat auditory cortex. eNeuro 5: ENEURO.0051-18.2018.

Cohen MR, Maunsell JH (2009) Attention improves performance primarily by reducing interneuronal correlations. Nat Neurosci 12:1594–1600.

Cohen MR, Maunsell JH (2010) A neuronal population measure of attention predicts behavioral performance on individual trials. J Neurosci 30:15241–15253.

Cohen MR, Kohn A (2011) Measuring and interpreting neuronal correlations. Nat Neurosci 14:811–819.

Darowski ES, Helder E, Zacks RT, Hasher L, Hambrick DZ (2008) Age-related differences in cognition: the role of distraction control. Neuropsychology 22:638–644.

David SV, Fritz JB, Shamma SA (2012) Task reward structure shapes rapid receptive field plasticity in auditory cortex. Proc Natl Acad Sci U S A 109:2144–2149.

De Luca A, Mambrini M, Conte Camerino D (1990) Changes in membrane ionic conductances and excitability characteristics of rat skeletal muscle during aging. Pflugers Arch 415:642–644.

Downer JD, Rapone B, Verhein J, O'Connor KN, Sutter ML (2017) Feature-selective attention adaptively shifts noise correlations in primary auditory cortex. J Neurosci 37:5378–5392.

Dubno JR, Dirks DD, Morgan DE (1984) Effects of age and mild hearing loss on speech recognition in noise. J Acoust Soc Am 76:87–96.

Dubno JR, Eckert MA, Lee FS, Matthews LJ, Schmiedt RA (2013) Classifying human audiometric phenotypes of age-related hearing loss from animal models. J Assoc Res Otolaryngol 14:687–701.

Ecker AS, Berens P, Tolias AS, Bethge M (2011) The effect of noise correlations in populations of diversely tuned neurons. J Neurosci 31:14272–14283.

Engle JR, Tinling S, Recanzone GH (2013) Age-related hearing loss in rhesus monkeys is correlated with cochlear histopathologies. PLoS One 8: e55092.

Fishman YI, Steinschneider M (2009) Temporally dynamic frequency tuning of population responses in monkey primary auditory cortex. Hear Res 254:64–76.

Fitzgibbons PJ, Gordon-Salant S (1996) Auditory temporal processing in elderly listeners. J Am Acad Audiol 7:183–189.

Fitzgibbons PJ, Gordon-Salant S (1998) Auditory temporal order perception in younger and older adults. J Speech Lang Hear Res 41:1052–1060.

Francis N, Mukherjee S, Kocillari L, Panzeri S, Babadi B, Kanold PO (2021) Sequential transmission of task-relevant information in cortical neuronal networks. bioRxiv. 2021.08.31.458395.

Francis NA, Winkowski DE, Sheikhattar A, Armengol K, Babadi B, Kanold PO (2018) Small networks encode decision-making in primary auditory cortex. Neuron 97:885–897.e6.

Frisina RD, Singh A, Bak M, Bozorg S, Seth R, Zhu X (2011) F1 (CBA × C57) mice show superior hearing in old age relative to their parental strains: Hybrid vigor or a new animal model for "Golden Ears"? Neurobiol Aging 32:17161724.

Fritz JB, Elhilali M, David SV, Shamma SA (2007) Auditory attention–focusing the searchlight on sound. Curr Opin Neurobiol 17:437–455.

Gao F, Wang G, Ma W, Ren F, Li M, Dong Y, Liu C, Liu B, Bai X, Zhao B, Edden RA (2015) Decreased auditory GABA+ concentrations in presbycusis demonstrated by edited magnetic resonance spectroscopy. Neuroimage 106:311–316.

Gold JR, Bajo VM (2014) Insult-induced adaptive plasticity of the auditory system. Front Neurosci 8:110.

Golob EJ, Mock JR (2019) Auditory spatial attention capture, disengagement, and response selection in normal aging. Atten Percept Psychophys 81:270–280.

Gopinath B, Rochtchina E, Wang JJ, Schneider J, Leeder SR, Mitchell P (2009) Prevalence of age-related hearing loss in older adults: Blue Mountains study. Arch Intern Med 169:415–416.

Gordon-Salant S, Fitzgibbons PJ (1995) Comparing recognition of distorted speech using an equivalent signal-to-noise ratio index. J Speech Hear Res 38:706–713.

Gordon-Salant S, Fitzgibbons PJ (1999) Profile of auditory temporal processing in older listeners. J Speech Lang Hear Res 42:300–311.

Gourévitch B, Edeline JM (2011) Age-related changes in the guinea pig auditory cortex: relationship with brainstem changes and comparison with tone-induced hearing loss. Eur J Neurosci 34:1953–1965.

Guizar-Sicairos M, Thurman ST, Fienup JR (2008) Efficient subpixel image registration algorithms. Opt Lett 33:156–158.

Harrison RV, Ibrahim D, Mount RJ (1998) Plasticity of tonotopic maps in auditory midbrain following partial cochlear damage in the developing chinchilla. Exp Brain Res 123:449–460.

He B, Lian J, Spencer KM, Dien J, Donchin E (2001) A cortical potential imaging analysis of the P300 and novelty P3 components. Hum Brain Mapp 12:120–130.

Henry KR, Chole RA (1980) Genotypic differences in behavioral, physiological and anatomical expressions of age-related hearing loss in the laboratory mouse. Audiology 19:369–383.

Holmstrom LA, Eeuwes LB, Roberts PD, Portfors CV (2010) Efficient encoding of vocalizations in the auditory midbrain. J Neurosci 30:802–819.

Hughes LF, Turner JG, Parrish JL, Caspary DM (2010) Processing of broadband stimuli across A1 layers in young and aged rats. Hear Res 264:79–85.

Kanold PO, Nelken I, Polley DB (2014) Local versus global scales of organization in auditory cortex. Trends Neurosci 37:502–510.

Kastner DB, Baccus SA, Sharpee TO (2015) Critical and maximally informative encoding between neural populations in the retina. Proc Natl Acad Sci U S A 112:2533–2538.

Kilgard MP, Merzenich MM (1998) Cortical map reorganization enabled by nucleus basalis activity. Science 279:1714–1718.

Kraft AW, Mitra A, Rosenthal ZP, Dosenbach NUF, Bauer AQ, Snyder AZ, Raichle ME, Culver JP, Lee JM (2020) Electrically coupled inhibitory interneurons constrain long-range connectivity of cortical networks. Neuroimage 215:116810.

Krukowski AE, Miller KD (2001) Thalamocortical NMDA conductances and intracortical inhibition can explain cortical temporal tuning. Nat Neurosci 4:424–430.

Kumar A, Thinschmidt JS, Foster TC (2019) Subunit contribution to NMDA receptor hypofunction and redox sensitivity of hippocampal synaptic transmission during aging. Aging (Albany NY) 11:5140–5157.

Las L, Stern EA, Nelken I (2005) Representation of Tone in Fluctuating Maskers in the Ascending Auditory System. J Neurosci 25:15031513.

Lee JY (2015) Aging and speech understanding. J Audiol Otol 19:7–13.

Leventhal AG, Wang Y, Pu M, Zhou Y, Ma Y (2003) GABA and its agonists improved visual cortical function in senescent monkeys. Science 300:812–815.

Liao C, Han Q, Ma Y, Su B (2016) Age-related gene expression change of GABAergic system in visual cortex of rhesus macaque. Gene 590:227–233.

Liguz-Lecznar M, Lehner M, Kaliszewska A, Zakrzewska R, Sobolewska A, Kossut M (2015) Altered glutamate/GABA equilibrium in aged mice cortex influences cortical plasticity. Brain Struct Funct 220:1681–1693.

Lin FR, Niparko JK, Ferrucci L (2011) Hearing loss prevalence in the United States. Arch Intern Med 171:1851–1853.

Ling LL, Hughes LF, Caspary DM (2005) Age-related loss of the GABA synthetic enzyme glutamic acid decarboxylase in rat primary auditory cortex. Neuroscience 132:1103–1113.

Lister J, Besing J, Koehnke J (2002) Effects of age and frequency disparity on gap discrimination. J Acoust Soc Am 111:2793–2800.

Liu J, Kanold PO (2021) Diversity of receptive fields and sideband inhibition with complex thalamocortical and intracortical origin in L2/3 of mouse primary auditory cortex. J Neurosci 41:3142–3162.

Liu J, Whiteway MR, Sheikhattar A, Butts DA, Babadi B, Kanold PO (2019) Parallel processing of sound dynamics across mouse auditory cortex via spatially patterned thalamic inputs and distinct areal intracortical circuits. Cell Rep 27:872–885.e7.

Llano DA, Turner J, Caspary DM (2012) Diminished cortical inhibition in an aging mouse model of chronic tinnitus. J Neurosci 32:16141–16148.

Malone BJ, Heiser MA, Beitel RE, Schreiner CE (2017) Background noise exerts diverse effects on the cortical encoding of foreground sounds. J Neurophysiol 118:1034–1054.

Maron ME (1961) Automatic indexing: an experimental inquiry. J ACM 8:404–417.

Martin del Campo HN, Measor KR, Razak KA (2012) Parvalbumin immunoreactivity in the auditory cortex of a mouse model of presbycusis. Hear Res 294:31–39.

Mendels OP, Shamir M (2018) Relating the structure of noise correlations in macaque primary visual cortex to decoder performance. Front Comput Neurosci 12:12.

Mendelson JR, Ricketts C (2001) Age-related temporal processing speed deterioration in auditory cortex. Hear Res 158:84–94.

Mendelson JR, Lui B (2004) The effects of aging in the medial geniculate nucleus: a comparison with the inferior colliculus and auditory cortex. Hear Res 191:21–33.

Meng X, Winkowski DE, Kao JPY, Kanold PO (2017) Sublaminar subdivision of mouse auditory cortex layer 2/3 based on functional translaminar connections. J Neurosci 37:10200–10214.

Milbrandt JC, Holder TM, Wilson MC, Salvi RJ, Caspary DM (2000) GAD levels and muscimol binding in rat inferior colliculus following acoustic trauma. Hearing Research 147:251–260.

Mitchell JF, Sundberg KA, Reynolds JH (2009) Spatial attention decorrelates intrinsic activity fluctuations in macaque area V4. Neuron 63:879–888.

Natan RG, Briguglio JJ, Mwilambwe-Tshilobo L, Jones SI, Aizenberg M, Goldberg EM, Geffen MN (2015) Complementary control of sensory adaptation by two types of cortical interneurons. Elife 4:

Nirenberg S, Latham PE (2003) Decoding neuronal spike trains: how important are correlations? Proc Natl Acad Sci U S A 100:7348–7353.

Occelli F, Hasselmann F, Bourien J, Eybalin M, Puel JL, Desvignes N, Wiszniowski B, Edeline JM, Gourévitch B (2019) Age-related changes in auditory cortex without detectable peripheral alterations: a multi-level study in Sprague-Dawley rats. Neuroscience 404:184–204.

Ouellet L, de Villers-Sidani E (2014) Trajectory of the main GABAergic interneuron populations from early development to old age in the rat primary auditory cortex. Front Neuroanat 8:40.

Parham K, Willott JF (1988) Acoustic startle response in young and aging C57BL/6J and CBA/J mice. Behav Neurosci 102:881–886.

Park SK, Lee SY, Kim DH, Lee MY, Oh SH (2019) Auditory cortical plasticity and reorganization in rats with single-sided deafness during early developmental period. Ann Otol Rhinol Laryngol 128:16S–25S.

Pasic TR, Moore DR, Rubel EW (1994) Effect of altered neuronal activity on cell size in the medial nucleus of the trapezoid body and ventral cochlear nucleus of the gerbil. J Comp Neurol 348:111–120.

Perez-Nieves N, Leung VCH, Dragott PL, Goodman DFM (2020) Neural heterogeneity promotes robust learning. bioRxiv 2020.12.18.423468.

Peters A, Sethares C, Luebke JI (2008) Synapses are lost during aging in the primate prefrontal cortex. Neuroscience 152:970–981.

Postma F, Liu CH, Dietsche C, Khan M, Lee HK, Paul D, Kanold PO (2011) Electrical synapses formed by connexin36 regulate inhibition- and experience-dependent plasticity. Proc Natl Acad Sci U S A 108:13770–13775.

Rabinowitz NC, Willmore BDB, King AJ, Schnupp JWH (2013) Constructing noise-invariant representations of sound in the auditory pathway. PLOS Biol 11:e1001710.

Reale RA, Brugge JF, Chan JC (1987) Maps of auditory cortex in cats reared after unilateral cochlear ablation in the neonatal period. Brain Res 431:281–290.

Recanzone G (2018) The effects of aging on auditory cortical function. Hear Res 366:99–105.

Renart A, de la Rocha J, Bartho P, Hollender L, Parga N, Reyes A, Harris KD (2010) The asynchronous state in cortical circuits. Science 327:587–590.

Robertson D, Irvine DR (1989) Plasticity of frequency organization in auditory cortex of guinea pigs with partial unilateral deafness. J Comp Neurol 282:456–471.

Rothschild G, Nelken I, Mizrahi A (2010) Functional organization and population dynamics in the mouse primary auditory cortex. Nat Neurosci 13:353–360.

Rupasinghe A, Francis N, Liu J, Bowen Z, Kanold PO, Babadi B (2021) Direct extraction of signal and noise correlations from two-photon calcium imaging of ensemble neuronal activity. Elife 10:e68046.

Scholl B, Gao X, Wehr M (2010) Nonoverlapping sets of synapses drive on responses and off responses in auditory cortex. Neuron 65:412–421.

Schuknecht HF, Gacek MR (1993) Cochlear pathology in presbycusis. Ann Otol Rhinol Laryngol 102:1–16.

Schneider DM, Woolley SMN (2013) Sparse and Background-Invariant Coding of Vocalizations in Auditory Scenes. Neuron 79:141152.

Shi L, Argenta AE, Winseck AK, Brunso-Bechtold JK (2004) Stereological quantification of GAD-67–immunoreactive neurons and boutons in the hippocampus of middle-aged and old Fischer 344 × Brown Norway rats. J Comp Neurol 478:282–291.

Sebastien De Landtsheer (2021) kmeans_opt. MATLAB Central File Exchange. Available at https://www.mathworks.com/matlabcentral/fileexchange/65823-kmeans_opt. Retrieved October 16, 2021.

Spongr VP, Flood DG, Frisina RD, Salvi RJ (1997) Quantitative measures of hair cell loss in CBA and C57BL/6 mice throughout their life spans. J Acoust Soc Am 101:35463553.

Stanley DP, Shetty AK (2004) Aging in the rat hippocampus is associated with widespread reductions in the number of glutamate decarboxylase-67 positive interneurons but not interneuron degeneration. J Neurochem 89:204–216.

Stanley EM, Fadel JR, Mott DD (2012) Interneuron loss reduces dendritic inhibition and GABA release in hippocampus of aged rats. Neurobiol Aging 33:431.e1–431.e13.

Sutter ML, Schreiner CE (1991) Physiology and topography of neurons with multipeaked tuning curves in cat primary auditory cortex. J Neurophysiol 65:1207–1226.

Teschner MJ, Seybold BA, Malone BJ, Hüning J, Schreiner CE (2016) Effects of signal-to-noise ratio on auditory cortical frequency processing. J Neurosci 36:2743–2756.

Tripathy SJ, Padmanabhan K, Gerkin RC, Urban NN (2013) Intermediate intrinsic diversity enhances neural population coding. Proc Natl Acad Sci U S A 110:8248–8253.

Trujillo M, Razak KA (2013) Altered cortical spectrotemporal processing with age-related hearing loss. J Neurophysiol 110:2873–2886.

Ulanovsky N, Las L, Farkas D, Nelken I (2004) Multiple time scales of adaptation in auditory cortex neurons. J Neurosci 24:10440–10453.

Wambacq IJ, Koehnke J, Besing J, Romei LL, Depierro A, Cooper D (2009) Processing interaural cues in sound segregation by young and middle-aged brains. J Am Acad Audiol 20:453–458.

Watkins PV, Kao JP, Kanold PO (2014) Spatial pattern of intra-laminar connectivity in supragranular mouse auditory cortex. Front Neural Circuits 8:15.

Willott JF, Parham K, Hunter KP (1988) Response properties of inferior colliculus neurons in young and very old CBA/J mice. Hear Res 37:1–14.

Willott JF, Parham K, Hunter KP (1991) Comparison of the auditory sensitivity of neurons in the cochlear nucleus and inferior colliculus of young and aging C57BL/6J and CBA/J mice. Hear Res 53:78–94.

Willott JF, Aitkin LM, McFadden SL (1993) Plasticity of auditory cortex associated with sensorineural hearing loss in adult C57BL/6J mice. J Comp Neurol 329:402–411.

Winkowski DE, Kanold PO (2013) Laminar transformation of frequency organization in auditory cortex. J Neurosci 33:1498–1508.

Winkowski DE, Bandyopadhyay S, Shamma SA, Kanold PO (2013) Frontal cortex activation causes rapid plasticity of auditory cortical processing. J Neurosci 33:18134–18148.

Winkowski DE, Nagode DA, Donaldson KJ, Yin P, Shamma SA, Fritz JB, Kanold PO (2018) Orbitofrontal cortex neurons respond to sound and activate primary auditory cortex neurons. Cereb Cortex 28:868–879.

Working Group on Speech Understanding and Aging, Committee on Hearing, Bioacoustics, and Biomechanics (1988) Speech understanding and aging. J Acoust Soc Am 83:859–895.